Accepted Manuscript

Oceanographic and climatic consequences of the tectonic evolution of the southern scotia sea basins, Antarctica

Lara F. Pérez, F. Javier Henández-Molina, Emanuele Lodolo, Fernando Bohoyo, Jesus Galindo-Zaldívar, Andrés Maldonado

PII: S0012-8252(18)30707-4
DOI: https://doi.org/10.1016/j.earscirev.2019.102922
Article Number: 102922
Reference: EARTH 102922

To appear in: *Earth-Science Reviews*

Received date: 8 December 2018
Revised date: 1 August 2019
Accepted date: 6 August 2019

Please cite this article as: L.F. Pérez, F.J. Henández-Molina, E. Lodolo, et al., Oceanographic and climatic consequences of the tectonic evolution of the southern scotia sea basins, Antarctica, Earth-Science Reviews, https://doi.org/10.1016/j.earscirev.2019.102922

OCEANOGRAPHIC AND CLIMATIC CONSEQUENCES OF THE TECTONIC EVOLUTION OF THE SOUTHERN SCOTIA SEA BASINS, ANTARCTICA

Lara F. Pérez[1]; F. Javier Henández-Molina[2]; Emanuele Lodolo[3]; Fernando Bohoyo[4]; Jesus Galindo-Zaldívar[5,6]; Andrés Maldonado[5]

1. British Antarctic Survey, High Cross, Madingley Road, Cambridge CB3 0ET, UK. **larrez@bas.ac.uk**

2. Department of Earth Sciences, Royal Holloway University of London, Egham Hill, Egham TW20 0EX, UK

3. Istituto Nazionale di Oceanografia e di Geofisica Sperimentale, Borgo Grotta Gigante 42/C, 34010 Sgonico (Trieste), Italy

4. Instituto Geologico y Minero de España, Rio Rosas 23, 28003 Madrid, Spain

5. Instituto Andaluz de Ciencias de la Tierra, Avd. de las Palmeras 4, 18100 Armilla (Granada) Spain

6. Dpto. Geodinámica, Granada University, Avd. de Fuentenueva s/n, 18002 Granada, Spain

Abstract

The Scotia Sea is a complex geological area located in the Southern Ocean which evolution is closely linked to the opening of the Drake Passage. Structural highs of continental nature derived from the former continental bridge between South America and the Antarctic Peninsula surround the abyssal plains of the Scotia Sea, restricting small isolated sedimentary basins along its southern margin. Morpho-structural and seismo-stratigraphic analyses of multichannel seismic reflection profiles, and additional geophysical data available in the region, have been conducted, decoding regional and global implications of the basins' evolution. The main aim of this work is to describe the stratigraphic evolution of the southern Scotia Sea basins, from their opening in the back-arc tectonic context of the Scotia Sea, to the last oceanographic changes which have carried on global climatic implications. The evolution of the south Scotia Sea occurred through two major tectonic stages registered in the sedimentary record of the region: 1) the end of the subduction in the northwest part of the Weddell Sea during the early Miocene, which shortened the back-arc subduction trench generating a major change in the regional tectonic field that determined the evolution of the southern basins towards two different types of passive margins: magma-poor and magma-rich; and 2) the full development of the southern Scotia Sea basins during the middle Miocene, that led to the opening of deep oceanic gateways along the South Scotia Ridge. Interplay among tectonics, oceanography and climate is proposed to control the regional sedimentary stacking pattern, with coeval changes globally identified.

Keywords: isolated oceanic basins, seismic stratigraphy, passive margins, paleoceanography, Drake Passage and Scotia Sea, Antarctica

1. Introduction

The relative movements between tectonic plates are mainly related to mantle activity, turning it to one of the most important forces shaping the Earth's surface (Potter and Szatmari, 2009; Lovell, 2010; Jones et al., 2012). Vast tectonic processes such as continental rifting and oceanic drifting set the primary background of the evolution of the sedimentary basins determining their long-term configuration, but also other short-term tectonic readjustments influence their stratigraphic architecture (Potter and Szatmari, 2009). To a similar extent, relative sea-level oscillations are caused by continental isostatic rebound related to magmatic activity or ice-cover balance (e.g., Maclennan and Lovell, 2002; Lovell, 2010; Vannucchi et al., 2013). Besides, tectonic uplift influences the ice sheet behaviour (e.g., Japsen et al., 2014). Environmental changes such as climate and sea-level variations represent short-term control factors that also influence sedimentary evolution (Hay, 1996; Hernández-Molina et al., 2014). Moreover, the action of deep and bottom currents determines the sedimentary distribution and shapes the seafloor, developing large Contourite Depositional Systems (e.g., Rebesco et al., 2014), while the oceanographic pattern influences the global climate and the ice sheets' oscillations in the long-term (e.g., Meredith et al., 2013).

The sedimentary record of the oceanic basins is therefore a function of the interaction of three major control factors: tectonics, oceanography and climate. The specific causal directionality of the relationships among them, their impact on deep-sea sedimentation, and the relative time scales on which they operate remain unclear. Further research on oceanic sedimentary basins is essential to resolve these questions (Hay, 1996; Hernández-Molina et al., 2014, 2016a). The Southern Ocean constitutes a key area to study the interaction among the major sedimentary control factors, since it presents a complex tectonic context; a very active oceanographic circulation; and the climatic oscillations accompanied drastic changes in the ice sheet evolution. Particularly, the sedimentary basins formed in the south Scotia Sea result from several tectonic phases and constitute major oceanographic gateways for the deep-water circulation, thus their evolution has had global climatic implications (Fig. 1; e.g., Dalziel et al., 2013a, 2013b; Eagles and Jokat, 2014).

The tectonic opening of the Drake Passage and the formation of the Scotia Sea paved the way for the onset of the present-day Global Thermohaline Circulation (Wunsch, 2002). Consequently, since its formation, the Scotia Sea is a key area for the interchange and interaction of deep-water masses between the Weddell Sea, the Pacific and the Atlantic oceans (Fig. 1; Lawver and Gahagan, 2003; Eagles and Jokat, 2014). A number of isolated sedimentary basins developed within the south Scotia Sea, to the north of the South Scotia Ridge (SSR; e.g., British Antarctic Survey, 1985). These small oceanic basins have had a major impact on deep-water circulation due to their role as main conduits for deep and bottom oceanographic currents (e.g., Tarakanov, 2012). A detailed understanding of the sedimentary record hosted by these basins is critical for documenting the tectonic influence on the development of the deep oceanographic pattern and its climatic implications.

The main aim of this study is to reveal the influence of tectonic evolution in the construction of the sedimentary record of isolated oceanic basins through its engage with oceanographic and climatic changes. To advance in the knowledge of the tectonic and stratigraphic evolution of the Scotia Sea, partial analysis of each one of the southern Scotia Sea basins have been regionally integrated here for first time, analysing the major tectonic events responsible of their evolution, and decoding the oceanographic and climatic events which shaped their stratigraphic architecture. The regional and global implications of the formation and evolution of these deep basins are highlighted and discussed.

2. Tectonic and oceanographic framework

The present-day, left-lateral motion between the large tectonic plates of South America and Antarctica is accommodated by two small tectonic plates (Fig. 1), the Scotia and Sandwich plates that form the Scotia Sea (Bohoyo et al., 2002; Smalley et al., 2003, 2007; Thomas et al., 2003; Eagles, 2010; Maestro et al., 2014; Eagles and Jokat, 2014). Embracing the oceanic crust of the Scotia Sea, the Scotia Arc is formed by continental fragments, once part of the continental bridge between South-America and the Antarctic Peninsula (e.g., Bohoyo et al., 2007). The western boundary of the Scotia Sea is formed by the Shackleton Fracture Zone, which forms a sinistral transpressive ridge crossing the Drake Passage (Geletti et al., 2005; Livermore et al., 2004). The back-arc development of the Scotia Sea was highly conditioned by the subduction of the Weddell Sea oceanic crust below the eastern margin of the Antarctic Peninsula and the South Orkney Microcontinent (SOM) (e.g., Barker, 1995; Bohoyo et al., 2002; Eagles and Jokat, 2014). The subduction of the Weddell Sea terminated between 22-19.5 Ma (Chron C6A-C6n) progressively to the East; when the South American–Antarctic ridge reached the continental margin forming the Endurance Collision Zone (Hamilton, 1989; Barker, 1984; 1995; Bohoyo et al., 2002; Livermore et al., 2005). Once the Endurance Collision Zone was formed, the active subduction was limited to the front of the arc along the South Sandwich Trench (Fig. 1), where the South American Plate is today thrusting below the Sandwich Plate (e.g., Dalziel et al., 2013b; Eagles and Jokat, 2014). The oceanic crust of the Scotia Sea has been formed by oceanic spreading along two main spreading centres, the relict West Scotia Ridge (WSR; 33-6.4 Ma; Maldonado et al., 2000; Bohoyo et al., 2016), and the presently-active East Scotia Ridge (ESR; 15-0 Ma; e.g., Larter et al., 2003). Both ridges are formed by several segments (Fig. 1), which have been active at different periods of time (Larter et al., 2003; Eagles et al., 2005). Volcanism in the central part of Scotia Sea formed the starfish and related volcanic edifices between 28.5 and 11.6 Ma (Dalziel et al., 2013b). In addition, a number of spreading centres have also created new oceanic crust behind the arc, forming the small basins of the south Scotia Sea (e.g., British Antarctic Survey, 1985; Eagles et al., 2006; Maldonado et al., 2006). They are, from west to east: Ona, Protector, Pirie (located slightly north), Dove and Scan basins (Fig. 1). The basins are bounded by bathymetric highs of continental nature and irregular shape, from west to east: Terror, Protector, Pirie, Bruce and Discovery banks (Fig. 2).

These basins are bounded to the south by the sinistral transcurrent fault system of the SSR, which constitutes the plate boundary between Scotia and Antarctic plates (Fig. 1). The northern boundary of the western and central SSR is defined by a reverse fault associated with local subduction that overthrusts the continental South Shetland Block over the oceanic crust of the Scotia Plate (Galindo-Zaldívar et al., 1996; Lodolo et al., 1997; Bohoyo et al., 2007; Civile et al., 2012). The active structures continue along the northern border of the SOM, where compressive structures are recognised and the South Orkney Trench traces the active oceanic-continental boundary (Maldonado et al., 1998; Bohoyo et al., 2007). In the eastern part of the SSR, structures and morphologies associated with convergence have been described; and strike-slip and normal faults produce a deep trough that may be interpreted as a pull-apart basin (e.g., Lodolo et al., 1997, 2010; Bohoyo et al., 2007).

The Scotia Sea, as part of the Drake Passage, is encompassed in the circumpolar Southern Ocean (Fig. 1; British Antarctic Survey, 1985). As a major oceanic gateway, the Drake Passage and the Scotia Sea, are key regions for the Global Thermohaline Circulation and therefore, for the Earth`s climatic system (Naveira-Garabato et al., 2007; Meredith et al., 2013). The Weddell Sea Deep Water (WSDW) goes through the SSR gateways from the Weddell Sea (Fig. 1), flowing across the Scotia Sea to the South Atlantic and South Pacific oceans and forming the most important component of the Antarctic Bottom Water (AABW), which is distributed worldwide and essential for the Global Thermohaline Circulation (e.g., Orsi et al., 1999). The absence of barriers to water flows around the Antarctic continent allows the vigorous eastward flow of the Antarctic Circumpolar Current (ACC; Orsi et al., 1999), which deeper fraction, the Circumpolar Deep Water (CDW) (Fig. 1), flows over the WSDW across the Scotia Sea (Naveira-Garabato et al., 2002).

3. Data and methods

Regional morpho-sedimentary and seismo-stratigraphic analyses were carried out to derive morphostructural and sediment thickness maps of the Scotia Sea based on a combined interpretation of the seismic profiles and the bathymetric background. The bathymetric data have been extracted from the Global Multi-Resolution Topography database (GMRT; Ryan et al., 2009) and the General Bathymetric Chart of the Oceans (GEBCO; Weatherall et al., 2015) including the International Bathymetric Chart of the Southern Ocean (IBCSO; Arndt et al., 2013). Most of the multichannel seismic profiles were acquired by the Spanish Antarctic Research Group during several expeditions carried out since 1992 (Fig. 2). This dataset has been integrated with open-access stack versions of internationally acquired profiles available at the Antarctic

Seismic Data Library System (SDLS). For the purposes of this study, the seismic interpretation was fostered by HIS Kingdom software following the interpretation criteria of basic analytical methods of seismic-stratigraphy (e.g., Payton, 1977).

Consequently, the major stratigraphic discontinuities were distinguished as high amplitude reflections that constitute local unconformities and present a regional signature. Major seismic units have been regionally correlated on the basis of their internal architecture and similarity of seismic facies. A detailed description of the seismic facies of the sedimentary record of each individual basin can be found in previous publications of the area (Maldonado et al., 1998, 2006, 2014; Bohoyo et al., 2007; Pérez et al., 2014a, 2014b, 2017), whereas in this work major regional features are described for the first time and a comparison is presented for a better understanding of the regional evolution. The age of the stratigraphic boundaries has been taken from previous works (Maldonado et al., 2006), estimated from the age of the underlying igneous crust based on models of magnetic anomalies, and in agreement with the sedimentation rates calculated in Jane Basin (Fig. 1) from the site 697 drilling during ODP Leg 113 (Gersonde et al., 1990). This site is located to the south of the Scotia Arc in the Antarctic Plate, but at the time of writing, it constitutes the drill-site closest to our study area with available chronostratigraphic information. According to these estimations the main stratigraphic discontinuities identified in the south Scotia Sea (called reflectors ‘g’ to ‘a’ in upwards stratigraphic order) were formed around 37, 33, 22, 14.9, 12.6, 6.4 and 3.8 Ma from bottom to top, as has been described in previous works (Maldonado et al., 2006, 2014; Pérez et al., 2014a, 2014b, 2017). New age models are expected to become available in the near future for the upper part of the sedimentary record of the Scotia Sea as outcomes of the recent drilling in the region during IODP Expedition 382. The bottom of the sedimentary record in the study area is hereafter referred to as basement top.

The thickness maps of the seismic units are the result of simple kriging interpolation between the profiles and allow to infer the regional distribution of sediments referred to each single unit or to the cluster of two or three units, referred to as packages. Both, thickness and depth of units and discontinuities are given in two-way travel-time (TWTT) due to the lack of an accurate seismic velocity model that would have allowed depth conversion. For descriptive purposes the southern Scotia Sea basins are differentiated as outer basins, Ona and Scan; and inner basins, Protector, Pirie and Dove (Fig. 1), according to their geographic location along the southern margin of the Scotia Arc.

4. Results

4.1 Regional structural features

The abyssal plains of the southern Scotia Sea basins are irregular in plan view, reaching an average water depth of 3500 m below sea-level (mbsl). The deepest abyssal plain is that in Dove Basin with around 4000 mbsl, whereas the shallowest is in Scan Basin with around 3000 mbsl (Fig. 3A, 3B, Table 1). The basins' sizes are less than 200 km E-W and 250 km N-S, with the exception of Ona Basin, which is more than 400 km E-W, considering the two sub-basins, located west and east of the central Ona High (Fig. 3A, 3B). On average within the basins, the basement top lies in a depth of ~6 s TWTT. However, the average depth of the basement top changes for each basin: Ona Basin 6-7.5 s TWTT; Protector Basin 6.5-7 s TWTT; Pirie Basin 5-6 s TWTT; Dove Basin 5.4-7.5 s TWTT; and Scan Basin 5-6 s TWTT (Fig. 3C, Table 1). The deepest depressions of the basement are observed in the outer basins. In Ona Basin the deepest depression reaches 7.8 s TWTT, and is roughly elongated N-S to the east of the Ona High (Fig. 3C). In Scan Basin the deepest depression reaches 6.6 s TWTT, is elongated NE-SW, and located in the southeast part of the basin. Below the basement top, the crust within the basins is characterised by high amplitude internal reflections typical of the igneous crust (Fig. 5). Tilted reflections dipping oceanwards are distinguished below the basement top of the outer basins (Fig. 4A). The deepest reflections below the basement top are identified between 7.5 and 9 s TWTT, with sparse distribution and little or no lateral continuity. They are referred to as Moho (Fig. 5).

In the outer basins, chaotic and hyperbolic seismic facies on the basement characterise the margins of Scan Basin and outcrop locally forming isolated mound morphologies in the Ona Basin (Fig. 5). These basins show gradual transitions to the surrounding banks where, in addition to normal faults, sparse reverse and strike-slip faults draw the boundaries between the abyssal plains and the surrounding highs. The margins of the inner basins are instead structured by several normal faults, which define blocks in the crust of the oceanic-continental transitional zone (Fig. 3A, 5). The fault throws decrease towards the abyssal plains as the blocks rotate and decrease in height. These margins are asymmetric in that the western slopes are steeper than the eastern slopes, while the eastern slopes are cut by a greater number of normal faults. In these basins the top of the chaotic igneous crust crops out locally to form roughly N-S trending ridges along the central axes of the basins (Fig. 5).

4.2 Regional stratigraphic considerations

The average sedimentary thickness in the southern Scotia Sea basins is about 1.5 s TWTT, however the thickness distribution is irregular (Fig. 3D). The outer basins present thicker sedimentary records (on average 2 s TWTT in Ona Basin and 1.8 s TWTT in Scan Basin) with several depocentres thicker than 2 s TWTT. Whereas the average thickness in the inner basins is above 1 s TWTT, with only a few depocentres exceeding 2 s TWTT (Fig. 3D, Table 1). The sediment thickness is therefore greater in the western and eastern outer basins of the south Scotia Sea, where up to eight seismic units can be distinguished. Only the five upper seismic units have been identified in the sedimentary record of the inner basins (Fig. 5).

Of the eight stratigraphic discontinuities that have been regionally distinguished (Reflector-g to Reflector-a upwards in the stratigraphic column), there are two that represent the major stratigraphic changes in the sedimentary record. Reflector-e and Reflector-c are widely distributed and recognizable, dividing the sedimentary record, and therefore the seismic units, into three major packages as described below (Fig. 6).

Package-3 is formed by the three lowermost units placed between the basement top and Reflector-e (seismic units VIII, VII and VI, from bottom to top; Fig. 5). It forms local isolated patches constrained to the main basement depressions of the outer basins, whereas it is absent from the inner basins (Fig. 6; Table 1). The patches reach thicknesses of over 0.8 s TWTT in the eastern part of Ona Basin and over 1 s TWTT in the southern part of Scan Basin. Among the units that form Package-3, Unit VIII is only identified along the axis of the main basement depression of the Ona Basin (Fig. 5). It is formed by a few reflections of high amplitude and low lateral continuity and has a thickness of 0.4 s TWTT. Above it, units VII and VI are also restricted by the basement morphology to the major depressions, but they are identified in both of the outer basins (Fig. 6). Unit VII is formed by a few high amplitude and lateral continuous reflections in Ona Basin, which appear more discontinuous in Scan Basin. Unit VII has a regional thickness of 0.5 s TWTT that reaches 1 s TWTT in the southern Scan Basin. The reflections that form Unit VI are of relatively lower amplitude and medium lateral continuity in both basins. The thickness of this unit reaches more than 0.4 s TWTT in the main depocentres.

Package-2 encompasses the seismic units located between Reflector-e and Reflector-c (seismic units V and IV, from bottom to top; Fig. 5). Package-2 is identified in all the basins of the south Scotia Sea, even though its distribution is constrained by the basement morphology. Major depocentres over 1 s TWTT in thickness are located in the eastern margins of the outer basins, whereas in the inner basins depocentres over 0.8 s TWTT in thickness are located at the western margins (Fig. 6). Unit V is the lowest unit identified in the deeper depressions of all the basins (Fig. 7). It is regionally formed by reflections of high to very high amplitude but low lateral continuity. Unit V forms small depocentres close to the margins of the basins (>0.4 s TWTT). The overlying unit, Unit IV, is formed by higher lateral continuity reflections, and fills more extensive depocentres (>0.6 s TWTT). In the easternmost basin, Scan Basin, mounded deposits are identified forming a major along-slope depocentre (>0.4 s TWTT). The widespread sedimentary distribution and major thickness of Unit IV relative to Unit V –with the exception of Protector Basin– is accompanied by a northward displacement of the depocentres, particularly in Ona Basin (Fig. 7).

Package-1 is formed by the three uppermost units identified above Reflector-c (units III, II and I, from bottom to top; Fig. 5). Package-1 is widespread and forms along-margin depocentres of over 1 s TWTT in the outer basins and over 0.8 s TWTT in the inner basins (Fig. 6). The three units of Package-1 are formed by reflections of high lateral continuity that in Unit III are tilted oceanwards along the basin margins (Fig. 4B). Widespread mounded and laminar bodies are identified within Package-1. The thickness of each individual unit is on average over 0.2 s TWTT, and in the major depocentres it exceeds 0.4 s TWTT (Fig. 7). Hence the sedimentary thickness of each of the three units is slightly less than the regional thickness of Unit IV (Fig. 7). From Unit III to Unit I there is a general trend for eastward displacement of the depocentres, in agreement with the overall distribution of sediments. The depocentres of Unit III are located in the southeastern areas of the basins, relatively westwards to these of the underlying unit, except in Protector Basin where they occupy its western side (Fig. 7). The depocentres of Unit II are located to the south in the eastern basins (from Scan Basin to Protector Basin), whereas they are placed in the northeast of the western basin (Ona Basin). In addition, Unit II presents a widespread distribution in the eastern basins whereas it is restricted to local depocentres in the western basin (Fig. 7). In Unit I, the major depocentres are located in the northern part of the eastern basins (Dove and Scan basins), whereas they are in the western side of Protector Basin and in the southeastern margin of Ona Basin (Fig. 7).

5. Discussion

5.1 Sedimentary basins structure and formation

The stratigraphic features and margin assembly observed in the southern Scotia Sea basins reveal marked differences between the structure of the outer – Ona and Scan – and inner – Protector, Pirie and Dove – basins (Fig. 3A). The outer basins present a shallower average water depth ranging from 3000 to 3500 mbsl (Fig. 3B). These basins hold the deepest depressions of the basement with a NE-SW trend (Fig. 3C). Even though, the extensional direction during the first steps of the Scotia Arc development is not precisely constrained, the orientations of these depressions correlates with the direction of the initial stages of the Drake Passage opening, which in turn was largely associated with a regional WNW-ESE tectonic extensional field (Fig. 8) (e.g., Lawver and Gahagan, 2003; Dalziel et al., 2013a, 2013b; Eagles and Jokat, 2014; Maldonado et al., 2014).

In the outer basins, volcanic intrusions and edifices identified from hyperbolic facies, chaotic bodies and basement highs, are widespread. In the Scan Basin, the oceanwards tilted reflections mimic the characteristics of the so-called seaward dipping reflectors largely associated with volcanic activity (Hinz, 1981). Volcanic build-ups have been identified in the bathymetry (Garcia et al., 2016). In the Ona Basin dredged samples point to the existence of isolated volcanoes (Maldonado et al., 2013), which have been also distinguished in the bathymetry (Bohoyo et al., 2016). These volcanic build-ups are more abundant along the margins of the basins, raising a smooth transition to the surrounding continental highs (Fig. 3A, 5). Dipping reflectors and marginal volcanic build-ups represent key elements defining magma-rich continental margins such as the Norwegian margin and generally the northern North Atlantic margins (Eldholm et al., 2000; Lundin et al., 2014), the Yelverton Bay in the Arctic Ocean (Funck et al., 2011), or the Argentinian margin in the South Atlantic Ocean (Paton et al., 2017). It is worth noting that the margins of the outer basins do not feature the classical continental blocks of typical rifting (Fig. 5), as in the well-known margins of the North Atlantic Ocean (e.g., Tucholke et al., 2007), but instead show fragmentation processes similar to those of the passive volcanic rifted margins, as occurred in most of the passive continental margins worldwide (Menzies et al., 2002). The lithospheric mantle of this kind of margins may have fragmented during breakup to produce extensive extrusive and intrusive magmatism from asthenosphere ascent during slow initial subsidence (e.g., Hinz, 1981; Eldholm et al., 2000; Franke et al., 2011). Rapid initial seafloor spreading is expected to follow the development of passive volcanic rifted margins (~50 mm/yr; Lundin et al., 2014), however the estimated initial spreading rates of the outer basins is relatively slow – 10 mm/yr in Ona Basin and 9 mm/yr in Scan Basin (Maldonado et al., 2014; Schreider et al., 2017, 2018). The beginning of the formation of Ona and Scan basins would have entailed crustal thinning and diffuse spreading, with abundant volcanic intrusions. The volcanic intrusions became progressively organised, in each basin constituting an ill-defined axial spreading centre that eventually was buried and became relict over time. Seafloor magnetic anomalies have been identified in the outer basins and interpreted in previous works (Maldonado et al., 2014; Schreider et al., 2017), although there are reasonable doubts about the nature of the igneous crust flooring the outer basins. The areas interpreted as oceanic crust from magnetic spreading anomalies may occasionally represent thinned continental lithosphere highly intruded by igneous rocks (Bronner et al., 2011; Franke et al., 2011; Dubinin et al., 2016).

The sedimentary record observed in the outer basins is thicker with respect to the inner basins and Package-3, formed of the three oldest units, is constrained to the outer basins (Fig. 3D, 6). Based on this, it is expected that the outer basins are relatively older age than the inner basins, being the first ones developed in the south Scotia Sea (Table 1). Some of the age models estimate dates of 44 and 35.7 Ma for the onset of the formation of Ona and Scan basins, respectively (Barker et al., 2013; Maldonado et al., 2014; Schreider et al., 2017). The Weddell Sea oceanic crust was subducting below the continental area formed by clustered blocks in the south of the Scotia Arc during this time (Barker, 1984; 1995). Within the back-arc context of the Scotia Sea (e.g., Dalziel et al., 2013a), the outer basins were located directly behind the subduction zone during their formation (Fig. 8). Thus, the subduction area was attached or nearby the forming basins providing volcanic and volcaniclastic material for the formation of their magma-rich passive continental margins. The magma production rate is one of the determining factors in the dynamic evolution of worldwide volcanic rifted margins which could evolve or not in an organized oceanic spreading system (Menzies et al., 2002).

The inner basins of the south Scotia Sea are deeper, between 3750 and 4000 mbsl (Fig. 3B). The basement top is deeper on average than in the outer basins, but it does not present large depressions (Fig. 3C). Protector and Dove basins have roughly N-S spreading centres (Eagles et al., 2006; Galindo-Zaldívar et al., 2006, 2014), locally outcropping at the seafloor indicating organized oceanic spreading (Fig. 5). Even if transtensional motion could be involved in the formation of these basins forming pull-apart structures (Pérez et al., 2017), they do not necessarily entail diffuse spreading as suggested by Dubinin et al. (2016). The margins of the inner basins are asymmetric and present a number of continental blocks fragmented by normal faults (Fig. 5), similar to those defined in magma-poor continental passive margins. Margins of the Baffin Bay, the Labrador Sea or off western Iberia constitute well-known examples of magma-poor continental extension and break-up (Chalmers and Pulvertaft, 2001; Whitmarsh et al., 2001). These margin features of the inner basins indicate development of the rift in a magma-poor context as consequence of lithospheric extension driven by far-field stresses. The rift of previously thinned continental crust could be reconstructed since the entire crust breaks up before exhumation of the mantle (Franke et al., 2011), and it is followed by the formation of the oceanic spreading centres. Isolated volcanic elements could have been emplaced in the inner basins as occurred in the magma-poor continental margins of South Australia and South China Sea (e.g., Reynolds et al., 2017), but they are the results of magmatic intrusions occurring after the cessation of seafloor spreading. The configuration of the margins and spreading centres of the inner basins suggests an E-W trending extensional context (Fig. 8), which is determined by the eastward elongation of the Scotia Arc (Barker, 2001).

The sedimentary record in the inner basins is thinner than in the outer basins, despite their deeper basement top (Fig. 3C, 3D), and only the two upper packages (packages -2 and -1) have been identified (Fig. 6). The thinner sedimentary record and the lower number of seismic units would suggest younger ages for the inner basins relative to the outer basins (Table 1). Despite the controversial age estimation (Barker et al., 2013; Bohoyo et al., 2007; Eagles et al., 2006; Galindo-Zaldívar et al., 2006; 2014), one of the models suggests ages of 17.4 Ma, 14.5 Ma and 22.8 Ma for the onset of formation of the Protector, Pirie and Dove basins respectively. These estimates would agree with later formation of the inner basins in a E-W extensional back-arc context (Fig. 8). During this later period, the back-arc subduction trench –the ancestral South Sandwich Trench– was restricted to the area east of Discovery Bank (Livermore et al., 1997; Dalziel et al., 2013a). The E-W extension of the Scotia Sea would have been driven by east-directed rollback of this trench (Fig. 8), similar to the present-day context in which the East Scotia Sea opens (e.g., Barker, 2001; Dalziel et al., 2013b; Maestro et al., 2014). Thus, the inner basins would have been located well to the west of the slab, and magma supply from its devolatilization would not have reached them, as samples collected along the Dove Basin ridge evidence (Galindo-Zaldívar et al., 2014).

5.2 Regional multi-phase rifting, drifting, and subsidence

The structural features identified in the sedimentary basins located along the southern margin of the Scotia Sea point to two markedly different tectonic settings during their formation and evolution. The major change in the evolutionary setting of these basins was intimately related to the regional change occurred in the back-arc system (Fig. 8). The initial stages of the Drake Passage opening and the Scotia Sea development accompanied subduction at a long trench in the northwest Weddell Sea and are recorded in the formation of the outer basins. The formation of the inner basins (Fig. 8, 9), was a response to a change occurred in the shape and length of the slab and trench caused by ridge crest-trench collisions off the South Orkney Microcontinent and Jane Bank (e.g., Barker et al., 1984). It has been suggested that strongly curved trenches are signals of subduction zones with narrow lengths of slab, which are able to migrate more easily within the mantle than wide slabs, giving rise to a tendency for faster trench rollback and accompanying back-arc spreading (Schellart et al., 2007). This mechanism may explain the different tectonic structures characterizing the inner and outer basins developed along the southern margin of the Scotia Sea. Consistent with this idea regional tectonic reconstructions show the ridge-trench collisions and formation of the Endurance Collision Zone started around 22 Ma (Barker, 1984, 1995; Hamilton, 1989; Livermore et al., 2005; Eagles and Jokat, 2014).

This major regional change in the tectonic regime is depicted by Reflector-e, which also records a major change in the sedimentary pattern of the southern Scotia Sea basins. Whereas Package-3, below Reflector-e, is only identified in the outer basins, the regionally identified Package-2, above Reflector-e, would have been deposited at the time of continental rifting which resulted in the formation and drifting of the inner basins (Fig. 10). The existence of five separate and different aged basins in the south Scotia Sea makes it an example of an area developed by multiple phases of rifting, such as the North Falkland Basin (Lohr and Underhill, 2015). In the North Falkland Basin, the end of the rifting phase of the Southern Rift Basin corresponded with the beginning of the syn-rift phase in the Northern Rift Basin (Lohr and Underhill, 2015). Likewise in the Scotia Sea the end of the syn-rift phase of the outer basins matched with the beginning of the syn-rift of the inner basins.

Considering the south Scotia Sea as a single-complex basin, Package-2 could represent the break-up sequence as defined by Soares et al (2012), like the transitional sequence that records the change from upper lithosphere breakup to the post-rift phase that led to the emplacement of normal oceanic crust (e.g., Welford et al., 2010; Soares et al., 2012). In this active tectonic context, the distribution of depocentres of the units forming Package-2, attached to the margins, points to down-slope sedimentary processes and continental sediment sources. The widespread distribution of a regionally thicker Unit IV with respect to a Unit V which is regionally thinner and patchy in the inner basins, reveals a higher sedimentation rate during Unit IV formation. The sediment source in Unit IV could be related to high tectonic instability that would enhance sedimentary deposition within the abyssal plains. The tectonic instabilities during Unit IV formation could be generated by the regional subsidence that followed the end of the oceanic spreading in the youngest southern Scotia Sea basins, Protector and Pirie (Fig. 8, 9). The subsidence is a result of the thermal subsidence following the rifting and drifting processes after the emplacement of magma (Davison and Underhill, 2011).

The end of the rifting and oceanic spreading in the inner basins of the southern Scotia Sea basins would be represented by the regional Reflector-c, which entails the second major change identified in the regional sedimentary record of the southern Scotia Sea basins (Fig. 10). The estimated age of this stratigraphic discontinuity is around 12.6 Ma according to regional models (Maldonado et al., 2006). The Reflector-c has been previously defined as a regional discontinuity in the Scotia Sea and the southern South Atlantic Ocean resulting from an oceanographic regional change (Maldonado et al., 2006; Pérez et al., 2014a, 2014b, 2015). The oceanographic change is denoted by the widespread distribution of contourite drifts and current-related features along the south Scotia Sea in the sedimentary record over the Reflector-c (i.e., Package-1 in our interpretation (Fig. 10)). The distribution of depocentres of the Package-1 units reflects a westward vs. eastward location of the basins with respect to the Drake Passage and the SSR gateways (Fig. 7), which control the regional oceanographic pattern. The evidence of widespread bottom current activity marked therefore the end of the continental break-up and oceanic spreading in the south Scotia Sea (Fig. 8, 9, 10), similar to what occurs in the phase of complete development of a margin according to Soares et al., (2014).

After the formation of Reflector-c, the tilted reflections observed along the basins's margins in Unit III reveal regional subsidence (Fig. 4B). The subsidence regionally registered in the Scotia Plate could be due to the subsidence of the upper plate in a convergent margin (Vannucchi et al., 2013) or regional thermal cooling. Deepening of the oceanic abyssal plains was also identified offshore Tierra del Fuego margin (Pérez et al., 2015) and even observed in several basins of the Northern Hemisphere (e.g., in the North Sea; Rasmussen et al., 2005). The global subsidence is associated with an increase of the orogenic activity in the main continental cordilleras (Potter and Szatmari, 2009) and a global decrease in the spreading rates of the major spreading centres in the Atlantic, Indian and Pacific oceans (between 19.4 and 9.8 Ma; Cogné and Humler, 2006). The increase in orogenic activity and the decrease of oceanic spreading were accompanied by a sedimentation rate peak in the three main oceans (Davies et al., 1977). Alternatively, the regional subsidence in the Scotia Sea could be related to regional cycles of uplift-subsidence driven by mantle convection effecting 2nd (10-80 Myr) and 3rd (1-10 Myr) order sea-level changes (Vail et al., 1977).

5.3 Oceanographic implications and global context

5.3.1 Early Miocene: CDW settlement

The regional change from NW-SE to E-W extension in the Scotia Arc marked by Reflector-e, activated the oceanic spreading along the W6 segment of the WSR (Fig. 8) (Eagles et al., 2005) and the opening of deep passages along the NSR, which settled the deep oceanographic connection between the Scotia Sea and the South Atlantic Ocean (Eagles and Jokat, 2014). CDW occupied the southern Scotia Sea abyssal plains slightly influencing the sedimentary distribution that otherwise was mostly controlled by the tectonic setting. Scattered current related features have been recorded in Package-2 revealing the regional eastward flow of CDW (Pérez et al., 2014a, 2014b, 2017). Regional tectonic changes occurred during the closure of the shallow Tierra del Fuego seaways at the end of the compressive period of the southern Andes (Torres Carbonell et al., 2014). On the contrary, the underthrusting of Indian Plate below Asian Plate began (Fig. 11), starting an uplift phase of the Himalayan Orogeny (Chatterjee et al., 2013). These phases of Antarctic extension and low-latitude compression occurred at the time of quiescence oceanic spreading in the Atlantic ridges and the Southwest Indian Ridge (Cogné and Humler, 2006). The regional tectonic setting is associated with an abrupt increase in Antarctic ice volume (Fig. 11). It occurred during the Oligocene-Miocene Transition (Greenop et al., 2019), when rapid change in the glaciation was favoured by the Earth's orbital parameters (e.g., Naish et al., 2001; Miller et al., 2005; Pälike et al., 2006) and declining atmospheric CO_2 below the critical threshold (Pagani et al., 2005; Greenop et al., 2019). Even though the chance of a Northern Hemisphere contribution to the ice budget is not discharged (e.g. Naish et al., 2001; Greenop et al., 2019), the Antarctic ice advance has been largely associated to the global drop in the sea-level (Miller et al., 2011). In addition we suggest that, the enhanced flow of CDW across Scotia Sea due to the circum-Antarctic passages opening facilitated the development of larger oceanographic water masses around Antarctica (Fig. 11).

5.3.2 Middle Miocene: AABW wax

Reflector-c regionally characterises a change in the oceanographic pattern (e.g., Maldonado et al., 2006). The sedimentary record of the Package-1 units infers a prevailing current towards the northwest associated with the flow of WSDW through the Scotia Sea abyssal plains once all the southern Scotia Sea basins and the SSR passages were fully opened (Pérez et al., 2014a, 2014b, 2017). To the north of the basins, South Georgia collided with the northeast Georgia Rise in relation to the cessation of the volcanism in the central part of Scotia Sea (Dalziel et al., 2013b), predating the opening of the eastern passages along the North Scotia Ridge (Eagles and Jokat, 2014). Reflector-c was formed around the time of the onset of the Central American Seaway shoaling (12 Ma; Nisancioglu et al., 2003) and the closure of the Indian Gateway (Hamon et al., 2013). The closure of these low-latitude gateways (Fig. 11), together with vertical re-adjustment in the Greenland-Scotland Ridge (e.g. Wright and Miller, 1996), let to the onset of a phase of enhanced Atlantic Meridional Overturning Circulation (Nisancioglu et al., 2003). The arrival of North Atlantic Deep Water (NADW) to southern latitudes led to waxing of the AABW (Carter and McCave, 1994) and consequently enhanced WSDW flow through the Scotia Sea (Fig. 11). The enhanced flow of WSDW forced the previously established CDW to a northern position in the Scotia Sea (Hernández-Molina et al., 2008). The northward flow of the AABW generated contourite terraces in the Argentinian and Uruguayan margins (Hernández-Molina et al., 2009, 2016b), and the development of mixed contouritic-turbiditic systems in the Brazilian margin (Contreras et al., 2010).

The stratigraphic discontinuity called Reflector-c has also been identified in the sedimentary record of the Weddell Sea and interpreted in terms of the onset of glacial conditions there (Maldonado et al., 2006; Lodolo et al., 2006; Hernández-Molina et al., 2008; Lindeque et al., 2013). The Antarctic Ice Sheet experienced large variability during early-middle Miocene times due to its high sensitivity to atmospheric oscillations and also favoured by the orbital configuration (Warny et al., 2009; Levy et al., 2016). Its maximum advance occurred during the Miocene Climate Transition (13.8 Ma) and persisted to 10 Ma (Levy et al., 2016), presenting stable marine-based ice sheets at the time of the Reflector-c formation. An erosive stratigraphic discontinuity referred to as 'Merlin', of similar age (13-10.5 Ma), has been identified along the western margins of the North Atlantic and correlated to the increased flux of NADW (e.g., Lear et al., 2003). Similarly, an erosional unconformity has been identified at the Brazilian margin (9-11 Ma; Contreras et al., 2010). At the time of the formation of these three stratigraphic discontinuities, the Transantarctic Mountains and the Shackleton Fracture Zone experienced an uplift phase (Fitzgerald, 1992; Livermore et al., 2004), which resulted in a northward shift in the polar front (McKay et al., 2012). The three stratigraphic discontinuities mark therefore reorganization in sedimentation-hiatus distribution patterns in significantly distant sedimentary basins as consequence of the enhancement of WSDW and its circulation towards the Scotia Sea, the northward migration of the CDW and the polar front, which involved the re-establishment of the Antarctic ice sheets and dropping of the global sea-level (Fig. 11) (Zachos et al., 2001; Miller et al., 2011) during the progression to cold polar climates (Wright et al., 1992).

6. Conclusions

The seismic stratigraphy of the south Scotia Sea allows to establish the relative sequence of formation and evolution of the oceanic basins located along its margin, despite the controversy in age models proposed by various authors. Two major events have conditioned the evolution of the southern Scotia Sea basins, leading to the formation of distinct outer and inner basins types. The older tectonic phase is associated with the end of the Weddell Sea subduction below the Scotia Plate. The outer basins formed during this first phase under a poorly defined extensional context. They constitute examples of magma-rich passive continental margins. The inner basins developed during a subsequent E-W extensional phase conditioned by shorting of the slab and trench by ride-trench collisions. They represent examples of magma-poor passive continental margins. The youngest regional tectonic change entailed the opening of gateways along the South Scotia Ridge and the completed formation of the basins – with the end of the continental rifting and oceanic spreading in the south Scotia Sea – involving a major change in the global oceanographic pattern with worldwide implications in the climatic system.

The regionally identified changes in the tectonic setting of the Scotia Sea were all part of global phases of intense plate tectonic activity, which involved, among others, changes in the major orogenic systems and oceanic spreading centres. They developed in configuration changes in the major oceanic gateways entailing worldwide oceanographic and climatic reorganization. There is a close relationship between the tectonic events and the oceanographic and climatic oscillations, particularly from the middle Miocene, which reveal clockwork interplay of these sedimentary control factors. Incoming results from IODP Expedition 382 are expected to improve the correlation between the major regional and global events, in particular providing an accurate chronostratigraphic model for the upper part of the sedimentary record.

Besides its global implications, the south Scotia Sea presents clear evidence of widespread bottom current activity marking the end of the continental break-up and oceanic spreading. The potential conceptual link between break-up, bottom current circulation and development of large contourites depositional and erosional features should be further explored in other areas.

Acknowledgements

The first author of this manuscript benefices of the Marie Skłodowska-Curie Action (MSCA) Global Fellowship H2020-MSCA-IF-GF-2017 no.: 792773 WAMSISE. This work was funded through projects CTM2011-30241-C01/02ANT and CTM2014-60451-C2-1/2, the special action CTM2011-13970-E, and is related to the project CTM2012-39599-C03. This work was also partially supported by the COMPASS consortium and performed in collaboration with the Continental Margins Research Group (CMRG) and The Drifters Research Group at Royal Holloway University of London (UK). We thank the Antarctic Seismic Data Library System for access to some of the data interpreted in this study. Our acknowledge to Dr. Gerhard Kuhn (Alfred-Wegener-Institut) and the anonymous reviewer that highly improve the initial version of this manuscript.

References

Arndt, J.E., Schenke, H.W., Martin, J., O., N.F., Gwen, B., Bruce, G., Michele, R., Fernando, B., Jongkuk, H., Jenny, B., Rudolf, G., Gleb, U., Felipe, B., Walter, R.-P., Morishita, T., Rochelle, W., 2013. The International Bathymetric Chart of the Southern Ocean (IBCSO) Version 1.0—A new bathymetric compilation covering circum-Antarctic waters. Geophysical Research Letters 40, 3111-3117.

Barker, P.F., 1995. Tectonic framework of the east Scotia Sea, in: Taylor, B. (Ed.), Backarc Basins: Tectonics and Magmatism. . Plenum, New York, pp. 281-314.

Barker, P.F., 2001. Evolution of the Scotia Sea region: Relevance to broad-band seismology. Terra Antartica 8, 67-70.

Barker, P.F., Barber, P.L., King, E.C., 1984. An early Miocene ridge crest-trench collision on the South Scotia Ridge near 36°W. Tectonophysics 102(1-4), 315-332.

Barker, P.F., Lawver, L.A., Larter, R.D., 2013. Heat-flow determinations of basement age in small oceanic basins of the southern central Scotia Sea, in: Hambrey, M.J., Barker, P.F., Barrett, P.J., Bowman, V., Davies, B., Smellie, J.L., Tranter, M. (Eds.), Antarctic Palaeoenvironments and Earth-Surface Pro. Geological Society, London, Special Publications, pp. 139-150.

Bohoyo, F., Galindo-Zaldívar, J., Jabaloy, A., Maldonado, A., Rodríguez-Fernández, J., Schreider, A., Suriñach, E., 2007. Extensional deformation and development of deep basins associated with the sinistral transcurrent fault zone of the Scotia–Antarctic plate boundary, in: Cunningham, W.D., Mann, P. (Eds.), Tectonics of Strike-Slip Restraining and Releasing Bends. Geological Society, London, Special Publications, pp. 203-217.

Bohoyo, F., Galindo-Zaldivar, J., Maldonado, A., Schreider, A.A., Suriñach, E., 2002. Basin development subsequent to ridge-trench collision: The Jane Basin, Antarctica. Marine Geophysical Research 23, 413-421.

Bohoyo, F., Larter, R.D., Galindo-Zaldivar, J., Leat, P.T., Maldonado, A., Tate, A.J., Gowland, E.J.M., Arndt, J.E., Dorschel, B., Kim, Y.D., Hong, J.K., Flexas, M.M., Lopez-Martinez, J., Maestro, A., Bermudez, O., Nitsche, F.O., Livermore, R.A., Riley, T.R., 2016. Bathymetry and geological setting of the Drake Passage (1: 1 500 000). BAS GEOMAP 2 Series. Cambridge, British Antarctic Survey.

British Antarctic Survey, C., 1985. Tectonic map of the Scotia Arc, in: British Antarctic Survey, C. (Ed.), Sheet (Misc) 3, p. Scale 1:3.000.000.

Bronner, A., Sauter, D., Manatschal, G., Péron-Pinvidic, G., Munschy, M., 2011. Magmatic breakup as an explanation for magnetic anomalies at magma-poor rifted margins. Nature Geoscience 4, 549-553.

Carter, L., McCave, I.N., 1994. Development of sediment drifts approaching an active plate margin under the SW Pacific deep western boundary current. Paleoceanography 9, 1061-1085.

Chalmers, J.A., Pulvertaft, T.C.R., 2001. Development of the continental margins of the Labrador Sea: A review, Geological Society Special Publication, pp. 77-105.

Chatterjee, S., Goswami, A., Scotese, C.R., 2013. The longest voyage: Tectonic, magmatic, and paleoclimatic evolution of the Indian plate during its northward flight from Gondwana to Asia. Gondwana Research 23, 238-267.

Civile, D., Lodolo, E., Vuan, A., Loreto, M.F., 2012. Tectonics of the Scotia-Antarctica plate boundary constrained from seismic and seismological data. Tectonophysics 550-553, 17-34.

Cogné, J.P., Humler, E., 2006. Trends and rhythms in global seafloor generation rate. Geochemistry, Geophysics, Geosystems 7, Q03011.

Contreras, J., Zühlke, R., Bowman, S., Bechstädt, T., 2010. Seismic stratigraphy and subsidence analysis of the southern Brazilian margin (Campos, Santos and Pelotas basins). Marine and Petroleum Geology 27, 1952-1980.

Dalziel, I.W.D., Lawver, L.A., Norton, I.O., Gahagan, L.M., 2013a. The Scotia Arc: Genesis, Evolution, Global Significance. Annual Review of Earth and Planetary Sciences 41, 767-793.

Dalziel, I.W.D., Lawver, L.A., Pearce, J.A., Barker, P.F., Hastie, A.R., Barfod, D.N., Schenke, H.W., Davis, M.B., 2013b. A potential barrier to deep Antarctic circumpolar flow until the late Miocene? Geology 41, 947-950.

Davies, T.A., Hay, W.W., Southam, J.R., Worsley, T.R., 1977. Estimates of Cenozoic oceanic sedimentation rates. Science 197, 53-55.

Davison, I., Underhill, J.R., 2011. Tectonics and Sedimentation in Extensional Rifts: Implications for Petroleum Systems, in: Gao, D. (Ed.), Tectonics and sedimentation: Implications for petroleum systems. AAPG Memoir, pp. 1-28.

Dubinin, E.P., Kokhan, A.V., Teterin, D.E., Grokhol'sky, A.L., Kurbatova, E.S., Sushchevskaya, N.M., 2016. Tectonics and types of riftogenic basins of the Scotia Sea, South Atlantic. Geotectonics 50, 35-53.

Eagles, G., 2010. The age and origin of the central Scotia Sea. Geophysical Journal International 183(2), 587-600.

Eagles, G., Jokat, W., 2014. Tectonic reconstructions for paleobathymetry in Drake Passage. Tectonophysics 611, 28-50.

Eagles, G., Livermore, R.A., Fairhead, J.D., Morris, P., 2005. Tectonic evolution of the West Scotia Sea. Journal of Geophysical Research B: Solid Earth 110, 1-19.

Eagles, G., Livermore, R.A., Morris, P., 2006. Small basins in the Scotia Sea: The Eocene Drake Passage gateway. Earth and Planetary Science Letters 242, 343-353.

Eldholm, O., Gladczenko, T.P., Skogseid, J., Planke, S., 2000. Atlantic volcanic margins: A comparative study, Geological Society Special Publication, pp. 411-428.

Fitzgerald, P.G., 1992. The Transantarctic Mountains of southern Victoria Land: The application of apatite fission track analysis to a rift shoulder uplift. Tectonics 11, 634-662.

Franke, D., Barckhausen, U., Baristeas, N., Engels, M., Ladage, S., Lutz, R., Montano, J., Pellejera, N., Ramos, E.G., Schnabel, M., 2011. The continent-ocean transition at the southeastern margin of the South China Sea. Marine and Petroleum Geology 28, 1187-1204.

Funck, T., Jackson, H.R., Shimeld, J., 2011. The crustal structure of the Alpha Ridge at the transition to the Canadian Polar Margin: Results from a seismic refraction experiment. Journal of Geophysical Research: Solid Earth 116.

Galindo-Zaldivar, J., Bohoyo, F., Maldonado, A., Schreider, A., Suriñach, E., Vázquez, J.T., 2006. Propagating rift during the opening of a small oceanic basin: The Protector Basin (Scotia Arc, Antarctica). Earth and Planetary Science Letters 241, 398-412.

Galindo-Zaldivar, J., Jabaloy, A., Maldonado, A., Sanz de Galdeano, C., 1996. Continental fragmentation along the South Scotia Ridge transcurrent plate boundary (NE Antarctic Peninsula). Tectonophysics 258, 275-301.

Galindo-Zaldívar, J., Puga, E., Bohoyo, F., González, F.J., Maldonado, A., Martos, Y.M., Pérez, L.F., Ruano, P., Schreider, A.A., Somoza, L., Suriñach, E., Díaz de Federico, A., 2014. Magmatism, structure and age of Dove Basin (Antarctica): A key to understanding South Scotia Arc development. Global and Planetary Change 122, 50-69.

García, M., Lobo, F.J., Maldonado, A., Hernández-Molina, F.J., Bohoyo, F., Pérez, L.F., 2016. High-resolution seismic stratigraphy and morphology of the Scan Basin contourite fan, southern Scotia Sea, Antarctica. Marine Geology 378, 361-373.

Geletti, R., Lodolo, E., Schreider, A.A., Polonia, A., 2005. Seismic structure and tectonics of the Shackleton Fracture Zone (Drake Passage, Scotia Sea). Marine Geophysical Researches 26 (1), 17-28.

Gersonde, R., Abelmann, A., Burckle, L.H., Hamilton, N., Lazarus, D., McCartney, K., O'Brien, P., Spieß, V., Wise, S.W.J., 1990. Biostratigraphic synthesis of neogene siliceous microfossils from the Antarctic Ocea, ODP LEG 113 (Weddell Sea), in: Barker, P.F., Kennett, J.P., al.", e. (Eds.), Proceedings of the Ocean Drilling Program Volume 113, Scientific Results. Sites 689-697. Ocean Drilling Program, College Station, Texas, pp. 915-936.

Greenop, R., Sosdian, S.M., Henehan, M.J., Wilson, P.A., Lear, C.H., Foster, G.L., 2019. Orbital forcing, ice-volume and CO_2 across the Oligocene-Miocene Transition. Paleoceanography and Paleoclimatology, doi: doi:10.1029/2018PA003420.

Hamilton, I.W., 1989. Geophysical Investigations of Subduction Related Processes in the Scotia Sea. University of Birmingham, Birmingham, UK.

Hamon, N., Sepulchre, P., Lefebvre, V., Ramstein, G., 2013. The role of eastern Tethys seaway closure in the Middle Miocene Climatic Transition (ca. 14 Ma). Climate of the Past 9, 2687-2702.

Hay, W.W., 1996. Tectonics and climate. Geol Rundsch 85, 409-437.

Hernández-Molina, F.J., Bohoyo, F., Galindo-Zaldívar, J., Jabaloy, A., Lobo, F.J., Lodolo, E., Maldonado, A., Medialdea, T., Rodríguez-Fernández, J., Somoza, L., Suriñach, E., Vázquez, J.T., 2008. Tectonic, sedimentary and paleoceanographic implications of a regional discontinuity (Reflector- c) in the Scotia and Weddell Seas (Antarctica). Geotemas 10, 1-4.

Hernández-Molina, F.J., Paterlini, M., Violante, R., Marshall, P., de Isasi, M., Somoza, L., Rebesco, M., 2009. Contourite depositional system on the Argentine Slope: An exceptional record of the influence of Antarctic water masses. Geology 37, 507-510.

Hernández-Molina, F.J., Sierro, F.J., Llave, E., Roque, C., Stow, D.A.V., Williams, T., Lofi, J., Van der Schee, M., Arnais, A., Ledesma, S., Rosales, C., Rodríguez-Tovar, F.J., Pardo-Igúzquiza, E., Brackenridge, R.E., 2016a. Evolution of the Gulf of Cadiz Margin and west Portugal contourite depositional system: tectonic, sedimentary and paleoceanographic implications from IODP Expedition 339. Marine Geology, 377: 7-39.

Hernández-Molina, F.J., Soto, M., Piola, A.R., Tomasini, J., Preu, B., Thompson, P., Badalini, G., Creaser, A., Violante, R.A., Morales, E., Paterlini, M., De Santa Ana, H., 2016b. A contourite depositional system along the Uruguayan continental margin: Sedimentary, oceanographic and paleoceanographic implications. Marine Geology 378, 333-349.

Hernandez-Molina, F.J., Stow, D.A., Alvarez-Zarikian, C.A., Acton, G., Bahr, A., Balestra, B., Ducassou, E., Flood, R., Flores, J.A., Furota, S., Grunert, P., Hodell, D., Jimenez-Espejo, F., Kim, J.K., Krissek, L., Kuroda, J., Li, B., Llave, E., Lofi, J., Lourens, L., Miller, M., Nanayama, F., Nishida, N., Richter, C., Roque, C., Pereira, H., Sanchez Goni, M.F., Sierro, F.J., Singh, A.D., Sloss, C., Takashimizu, Y., Tzanova, A., Voelker, A., Williams, T., Xuan, C., 2014. Paleoceanography. Onset of Mediterranean outflow into the North Atlantic. Science 344, 1244-1250.

Hinz, K., 1981. Hypothesis on terrestrial catastrophes: wedges of very thick oceanward dipping layers beneath passive continental margins - their origins and paleoenvironmental significance. Geologisches Jahrbuch, Series E 22, 1-28.

Japsen, P., Green, P.F., Bonow, J.M., Nielsen, T.F.D., Chalmers, J.A., 2014. From volcanic plains to glaciated peaks: Burial, uplift and exhumation history of southern East Greenland after opening of the NE Atlantic. Global and Planetary Change 116, 91-114.

Jones, S.M., Lovell, B., Crosby, A.G., 2012. Comparison of modern and geological observations of dynamic support from mantle convection. Journal of the Geological Society 169, 745-758.

Kominz, M.A., Browning, J.V., Miller, K.G., Sugarman, P.J., Mizintseva, S., Scotese, C.R., 2008. Late Cretaceous to Miocene sea-level estimates from the New Jersey and Delaware coastal plain coreholes: An error analysis. Basin Research 20, 211-226.

Larter, R.D., Vanneste, L.E., Morris, P., Smythe, D.K., 2003. Structure and tectonic evolution of the South Sandwich arc, in: Larter, R.D., Leat, P.T. (Eds.), Intra-Oceanic Subduction Systems: Tectonic and Magmatic Processes. Geological Society, London, Special Publications, London, pp. 255-284.

Lawver, L.A., Gahagan, L.M., 2003. Evolution of cenozoic seaways in the circum-antarctic region. Palaeogeography, Palaeoclimatology, Palaeoecology 198, 11-37.

Lear, C.H., Rosenthal, Y., Wright, J.D., 2003. The closing of a seaway: Ocean water masses and global climate change. Earth and Planetary Science Letters 210, 425-436.

Levy, R., Harwood, D., Florindo, F., Sangiorgi, F., Tripati, R., Von Eynatten, H., Gasson, E., Kuhn, G., Tripati, A., DeConto, R., Fielding, C., Field, B., Golledge, N., McKay, R., Naish, T., Olney, M., Pollard, D., Schouten, S., Talarico, F., Warny, S., Willmott, V., Acton, G., Panter, K., Paulsen, T., Taviani, M., 2016. Antarctic ice sheet sensitivity to atmospheric CO_2 variations in the early to mid-Miocene. Proceedings of the National Academy of Sciences of the United States of America 113, 3453-3458.

Lindeque, A., Martos Martin, Y.M., Gohl, K., Maldonado, A., 2013. Deep-sea pre-glacial to glacial sedimentation in the Weddell Sea and southern Scotia Sea from a cross-basin seismic transect. Marine Geology 336, 61-83.

Livermore, R., Balanyá, J.C., Maldonado, A., Martínez, J.M., Rodríguez-Fernández, J., Sanz de Galdeano, C., Zaldivar, J.G., Jabaloy, A., Barnolas, A., Somoza, L., Hernández-Molina, J., Suriñach, E., Viseras, C., 2000. Autopsy on a dead spreading center: The Phoenix Ridge, Drake Passage, Antarctica. Geology 28, 607-610.

Livermore, R., Cunningham, A., Vanneste, L., Larter, R., 1997. Subduction influence on magma supply at the East Scotia Ridge. Earth and Planetary Science Letters 150, 261-275.

Livermore, R., Eagles, G., Morris, P., Maldonado, A., 2004. Shackleton Fracture Zone: No barrier to early circumpolar ocean circulation, Geology, 32(9), 797-800.

Livermore, R., Nankivell, A., Eagles, G., Morris, P., 2005. Paleogene opening of Drake Passage. Earth and Planetary Science Letters 236, 459-470.

Lodolo, E., Coren, F., Schreider, A.A., Ceccone, G., 1997. Geophysical evidence of a relict oceanic crust in the southwestern Scotia Sea. Marine Geophysical Research 19, 439-450.

Lodolo, E., Donda, F., Tassone, A., 2006. Western Scotia Sea margins: Improved constraints on the opening of the Drake Passage. Journal of Geophysical Research B: Solid Earth 111, B06101.

Lodolo, E., Civile, D., Vuan, A., Tassone, A., Geletti, R., 2010. The Scotia-Antarctica plate boundary from 35°W to 45°W. Earth and Planetary Science Letters 293 1-2, 200-215.

Lohr, T., Underhill, J.R., 2015. Role of rift transection and punctuated subsidence in the development of the North Falkland Basin. Petroleum Geoscience 21, 85-110.

Lovell, B., 2010. A pulse in the planet: Regional control of high-frequency changes in relative sea level by mantle convection. Journal of the Geological Society 167, 637-648.

Lundin, E., Redfield, T., Peron-Pindivic, G., 2014. Rifted continental margins: Geometric influence on crustal architecture and melting, in: Pindell, J., Horn, B., Rosen, N., Weimer, P., Dinkleman, M., Lowrie, A., Fillon, R., Granath, J., Kennan, L. (Eds.), Sedimentary Basins: Origin, Depositional Histories, and Petroleum Systems. SEPM Society for Sedimentary Geology.

Maclennan, J., Lovell, B., 2002. Control of regional sea level by surface uplift and subsidence caused by magmatic underplating of Earth's crust. Geology 30, 675-678.

Maestro, A., López-Martínez, J., Galindo-Zaldívar, J., Bohoyo, F., Mink, S., 2014. Evolution of the stress field in the southern Scotia Arc from the late Mesozoic to the present-day. Global and Planetary Change 123(B), 269-297.

Maldonado, A., Acosta, A., García, M., Lobo, F.J., Martos, Y., Pérez, L.F., Puga, E., Bohoyo, F., Casas, D., González, F.J., León, R., Medialdea, T., Somoza, L., Galindo-Zaldivar, J., Larrad-Revuelto, M., Rey-Díaz de Rada, J., Bozzano, G., Elizondo, M.E., Esteban, F., Pelzmajer, M., 2013. Dredged rock samples from the southwestern Scotia Sea (SCAN 2013): remnants from the South America-Antarctic continental bridge. Bollettino di Geofisica teorica ed applicada 54 (2), 330-333.

Maldonado, A., Balanyá, J.C., Barnolas, A., Galindo-Zaldivar, J., Hernández, J., Jabaloy, A., Livermore, R., Martínez-Martínez, J.M., Rodríguez-Fernández, J., De Galdeano, C.S., Somoza, L., Surinach, E., Viseras, C., 2000. Tectonics of an extinct ridge-transform intersection, Drake Passage (Antarctica). Marine Geophysical Research 21, 43-67.

Maldonado, A., Bohoyo, F., Galindo-Zaldívar, J., Hernández-Molina, F.J., Jabaloy, A., Lobo, F.J., Rodríguez-Fernández, J., Suriñach, E., Vázquez, J.T., 2006. Ocean basins near the Scotia - Antarctic plate boundary: Influence of tectonics and paleoceanography on the Cenozoic deposits. Marine Geophysics Research 27 (2), 83-107.

Maldonado, A., Bohoyo, F., Galindo-Zaldívar, J., Hernández-Molina, F.J., Lobo, F.J., Lodolo, E., Martos, Y.M., Pérez, L.F., Schreider, A.A., Somoza, L., 2014. A model of oceanic development by ridge jumping: Opening of the Scotia Sea. Global and Planetary Change 123, 152-173.

Maldonado, A., Zitellini, N., Leitchenkov, G., Balanyá, J.C., Coren, F., Galindo-Zaldivar, J., Lodolo, E., Jabaloy, A., Zanolla, C., Rodríguez-Fernández, J., Vinnikovskaya, O., 1998. Small ocean basin development along the Scotia-Antarctica plate boundary and in the northern Weddell Sea. Tectonophysics 296, 371-402.

McKay, R., Naish, T., Carter, L., Riesselman, C., Dunbar, R., Sjunneskog, C., Winter, D., Sangiorgi, F., Warren, C., Pagani, M., Schouten, S., Willmott, V., Levy, R., DeConto, R., Powell, R.D., 2012. Antarctic and Southern Ocean influences on Late Pliocene global cooling. Proceedings of the National Academy of Sciences of the United States of America 109, 6423–6428.

Menzies, M.A., Klemperer, S.L., Ebinger, C.J., Baker, J., 2002. Characteristics of volcanic rifted margins, Special Paper of the Geological Society of America, pp. 1-14.

Meredith, M.P., Brown, P.J., Naveira Garabato, A.C., Jullion, L., Venables, H.J., Messias, M.-J., 2013. Dense bottom layers in the Scotia Sea, Southern Ocean: Creation, lifespan, and destruction. Geophysical Research Letters 40, 933-936.

Miller, K., Mountain, G., Wright, J., Browning, J., 2011. A 180-Million-Year Record of Sea Level and Ice Volume Variations from Continental Margin and Deep-Sea Isotopic Records. Oceanography 24, 40-53.

Miller, K.G., Rowley, D.B., Kominz, M.A., Kent, D.V., 2005. Seafloor spreading, sea level, and ocean chemistry changes. Eos 86, 335.

Naish, T.R., Woolfe, K.J., Barrett, P.J., Wilson, G.S., Atkins, C., Bohaty, S.M., Bucker, C.J., Claps, M., Davey, F.J., Dunbar, G.B., Dunn, A.G., Fielding, C.R., Florindo, F., Hannah, M.J., Harwood, D.M., Henrys, S.A., Krissek, L.A., Lavelle, M., van der Meer, J., McIntosh, W.C., Niessen, F., Passchier, S., Powell, R.D., Roberts, A.P., Sagnotti, L., Scherer, R.P., Strong, C.P., Talarico, F., Verosub, K.L., Villa, G., Watkins, D.K., Webb, P.-N., Wonik, T., 2001. Orbitally induced oscillations in the East Antarctic ice sheet at the Oligocene/Miocene boundary. Nature 413, 719-723.

Naveira Garabato, A.C., McDonagh, E.L., Stevens, D.P., Heywood, K.J., Sanders, R.J., 2002. On the export of Antarctic Bottom Water from the Weddell Sea. Deep-Sea Research Part II: Topical Studies in Oceanography 49, 4715-4742.

Naveira-Garabato, A.C., Stevens, D.P., Watson, A.J., Roether, W., 2007. Short-circuiting of the overturning circulation in the Antarctic Circumpolar Current. Nature 447, 194-197.

Nisancioglu, K.H., Raymo, M.E., Stone, P.H., 2003. Reorganization of Miocene deep water circulation in response to the shoaling of the Central American Seaway. Paleoceanography 18, 1006.

Orsi, A.H., Johnson, G.C., Bullister, J.L., 1999. Circulation, mixing, and production of Antarctic Bottom Water. Progress in Oceanography 43, 55-109.

Orsi, A.H., Whitworth III, T., Nowlin Jr, W.D., 1995. On the meridional extent and fronts of the Antarctic Circumpolar Current. Deep-Sea Research Part I 42, 641-673.

Pagani, M., Zachos, J.C., Freeman, K.H., Tipple, B., Bohaty, S., 2005. Atmospheric science: Marked decline in atmospheric carbon dioxide concentrations during the Paleogene. Science 309, 600-603.

Pälike, H., Norris, R. D., Herrle, J. O., Wilson, P. A., Coxall, H. K., Lear, C. H., Shackleton, N. J., Tripati, A. K., and Wade, B. S. (2006), The Heartbeat of the Oligocene Climate System. Science 314 (5807), 1894-1898.

Paton, D.A., Pindell, J., McDermott, K., Bellingham, P., Horn, B., 2017. Evolution of seaward-dipping reflectors at the onset of oceanic crust formation at volcanic passive margins: Insights from the South Atlantic. Geology 45, 439-442.

Payton, C.E., 1977. Seismic stratigraphy-applications to hydrocarbon exploration. American Association of Petroleum geologists, Tulsa, Okla.

Pérez, L.F., Hernández-Molina, F.J., Esteban, F.D., Tassone, A., Piola, A.R., Maldonado, A., Preu, B., Violante, R.A., Lodolo, E., 2015. Erosional and depositional contourite features at the transition between the western Scotia Sea and southern South Atlantic Ocean: links with regional water-mass circulation since the Middle Miocene. Geo-Marine Letters 35, 271-288.

Pérez, L.F., Lodolo, E., Maldonado, A., Hernández-Molina, F.J., Bohoyo, F., Galindo-Zaldívar, J., Lobo, F.J., Burca, M., 2014a. Tectonic development, sedimentation and paleoceanography of the Scan Basin (southern Scotia Sea, Antarctica). Global and Planetary Change 123, 344-358.

Pérez, L.F., Maldonado, A., Bohoyo, F., Hernández-Molina, F.J., Vázquez, J.T., Lobo, F.J., Martos, Y.M., 2014b. Depositional processes and growth patterns of isolated oceanic basins: the Protector and Pirie basins of the Southern Scotia Sea (Antarctica). Marine Geology 357, 163-181.

Pérez, L.F., Maldonado, A., Hernández-Molina, F.J., Lodolo, E., Bohoyo, F., Galindo-Zaldívar, J., 2017. Tectonic and oceanographic control of sedimentary patterns in a small oceanic basin: Dove Basin (Scotia Sea, Antarctica). Basin Research 29, 255-276.

Potter, P.E., Szatmari, P., 2009. Global Miocene tectonics and the modern world. Earth-Science Reviews 96, 279-295.

Rasmussen, E.S., VejbæK, O.V., Bidstrup, T., Piasecki, S., DybkjæR, K., 2005. Late Cenozoic depositional history of the Danish North sea basin: Implications for the petroleum systems in the Kraka, Halfdan, Siri and Nini fields, Petroleum Geology Conference Proceedings, pp. 1347-1358.

Rebesco, M., Hernández-Molina, F.J., Van Rooij, D., Wåhlin, A., 2014. Contourites and associated sediments controlled by deep-water circulation processes: state of the art and future considerations. Marine Geology 352, 111-154.

Reynolds, P., Holford, S., Schofield, N., Ross, A., 2017. The shallow depth emplacement of mafic intrusions on a magma-poor rifted margin: An example from the Bight Basin, southern Australia. Marine and Petroleum Geology 88, 605-616.

Ryan, W.B.F., Carbotte, S.M., Coplan, J.O., O'Hara, S., Melkonian, A., Arko, R., Weissel, R.A., Ferrini, V., Goodwillie, A., Nitsche, F., Bonczkowski, J., Zemsky, R., 2009. Global multi-resolution topography synthesis. Geochemistry, Geophysics, Geosystems 10(3).

Rodríguez-Fernández, J., Balanyá, J. C., Galindo-Zaldivar, J., and Maldonado, A., 1997. Tectonic evolution of a restricted ocean basin: the Powell Basin (northeastern Antarctic Peninsula). Geodinamica Acta 10 (4), 159-174.

Schellart, W.P., Freeman, J., Stegman, D.R, Moresi, L., May, D., 2007. Evolution and diversity of subduction zones controlled by slab width. Nature 446, 308–311.Schreider, Al.A., Schreider, A.A., Galindo-Zaldivar, J., Maldonado, A., Sazhneva, A.E., Evsenko, E.I., 2017. Age of the Scan Basin (Scotia Sea). Oceanology 57, 328-336.

Schreider, A.A., Schreider, A.A., Sazhneva, A.E., Galindo-Zaldivar, J., Ruano, P., Maldonado, A., Martos-Martin, Y., Lobo, F., 2018. Structure of Subsurface Sediments in the Scan Basin (Scotia Sea). Oceanology 58, 133-136.

Smalley, R., Dalziel, I.W.D., Bevis, M.G., Kendrick, E., Stamps, D.S., King, E.C., Taylor, F.W., Lauría, E., Zakrajsek, A., Parra, H., 2007. Scotia arc kinematics from GPS geodesy. Geophysical Research Letters 34(21), doi:10.1029/2002GC000446.

Smalley Jr, R., Kendrick, E., Bevis, M.G., Dalziel, I.W.D., Taylor, F., Lauría, E., Barriga, R., Casassa, G., Olivero, E., Piana, E., 2003. Geodetic determination of relative plate motion and crustal deformation across the Scotia-South America plate boundary in eastern Tierra del Fuego. Geochemistry, Geophysics, Geosystems 4(9), doi:10.1029/2007GL031699.

Soares, D.M., Alves, T.M., Terrinha, P., 2012. The breakup sequence and associated lithospheric breakup surface: Their significance in the context of rifted continental margins (West Iberia and Newfoundland margins, North Atlantic). Earth and Planetary Science Letters 355-356, 311-326.

Soares, D.M., Alves, T.M., Terrinha, P., 2014. Contourite drifts on early passive margins as an indicator of established lithospheric breakup. Earth and Planetary Science Letters 401, 116-131.

Tarakanov, R.Y., 2012. The Scotia Sea and the Drake Passage as an orographic barrier for the Antarctic Circumpolar Current. Oceanology 52, 157-170.

Thomas, C., Livermore, R., Pollitz, F., 2003. Motion of the Scotia sea plates. Geophysical Journal International 155(3), 789-804.

Torres Carbonell, P.J., Dimieri, L.V., Olivero, E.B., Bohoyo, F., Galindo-Zaldívar, J., 2014. Structure and tectonic evolution of the Fuegian Andes (southernmost South America) in the framework of the Scotia Arc development. Global and Planetary Change.

Tucholke, B.E., Sawyer, D.S., Sibuet, J.C., 2007. Breakup of the Newfoundland-Iberia rift, in: Karner, G.D., Manatschal, G., Pinheiro, L.M. (Eds.), Imaging, Mapping and Modelling Continental Lithosphere Extension and Breakup. Geological Society Special Publication, pp. 9-46.

Vail, P.R., Mitchum, R.M., Thompson, S., 1977. Seismic stratigraphy and global changes of sea level, Part 3—Relative changes of sea level from coastal onlap. AAPG Memoir 26, 63-81.

Vannucchi, P., Sak, P.B., Morgan, J.P., Ohkushi, K., Ujiie, K., 2013. Rapid pulses of uplift, subsidence, and subduction erosion offshore Central America: Implications for building the rock record of convergent margins. Geology 41, 995-998.

Warny, S., Askin, R. A., Hannah, M. J., Mohr, B. A. R., Raine, J. I., Harwood, D. M., Florindo, F., and the SMS Science Team, 2009. Palynomorphs from a sediment core reveal a sudden remarkably warm Antarctica during the middle Miocene. Geology 37, 955-958.

Weatherall, P., M., M.K., Martin, J., Thierry, S., Shin, T., Erik, A.J., Marzia, R., Dale, C., Vicki, F., Rochelle, W., 2015. A new digital bathymetric model of the world's oceans. Earth and Space Science 2, 331-345.

Welford, J.K., Smith, J.A., Hall, J., Deemer, S., Srivastava, S.P., Sibuet, J.C., 2010. Structure and rifting evolution of the northern Newfoundland Basin from erable multichannel seismic reflection profiles across the southeastern margin of Flemish Cap. Geophysical Journal International 180, 976-998.

Whitmarsh, R.B., Manatschal, G., Minshull, T.A., 2001. Evolution of magma-poor continental margins from rifting to seafloor spreading. Nature 413, 150.

Wright, J.D., Miller, K.G., 1996. Control of North Atlantic Deep Water circulation by the Greenland-Scotland Ridge. Paleocoanography 11, 157-170.

Wright, J.D., Miller, K.G., Fairbanks, R.G., 1992. Early and Middle Miocene stable isotopes: Implications for Deepwater circulation and climate. Paleoceanography 7, 357-389.

Wunsch, C., 2002. Oceanography: What is the thermohaline circulation? Science 298.

Zachos, J., Pagani, H., Sloan, L., Thomas, E., Billups, K., 2001. Trends, rhythms, and aberrations in global climate 65 Ma to present. Science 292, 686-693.

Zachos, J.C., Dickens, G.R., Zeebe, R.E., 2008. An early Cenozoic perspective on greenhouse warming and carbon-cycle dynamics. Nature 451, 279-283.

Table 1.- Summary of the main features of the south Scotia Sea sedimentary basins. Estimated age is according to previous published models: Barker et al., 2013; Galindo-Zaldívar et al., 2006; 2014; Maldonado et al., 2014; Schreider et al., 2017).

	Outer Basins: Type I		***Inner Basins: Type II***	
	Ona	**Scan**	**Protector**	**Dove**
Morphology	Irregular	Irregular	Triangular	Sigmoidal
Seafloor average depth	3000 – 3500 m		3750 – 4000 m	
Basement average depth	6-7.5 s TWTT	5-6 s TWTT	6.5-7 s TWTT	5.4-7.5 s TWTT
Dipping reflectors	Yes		No	
Estimated Age	44 Ma	35.7 Ma	17.4 Ma	22.8 Ma
Sedimentary Record Thickness	3.5 s TWTT	1.8 s TWTT	0.8 s TWTT	1 s TWTT
Number of Seismic Units	8	7	5	
Volcanic Margin	No	Yes	No	
Inside Volcanism	Widespread		No	Local

Figure 1.- Simplified bathymetric map of the Scotia Sea derived from the new digital bathymetric model of the world's oceans (Weatherall et al., 2015). Tectonic setting of the Scotia Sea (modified from Bohoyo et al., 2007). 1, transform fault; 2, active transcurrent fault; 3, inactive subduction zone; 4, active subduction zone; 5, active extensional zone; 6, active spreading centre; 7, inactive spreading centre; 8, continental-oceanic crust boundary. Morphological and oceanographic features: AP, Antarctic Peninsula; BS, Bransfield Strait; DB, Dove Basin; EFZ, Endurance Fracture Zone; EI, Elephant Island; JB, Jane Basin; OB, Ona Basin; PB, Powell Basin; PiB, Pirie Basin; PrB, Protector Basin; SB, Scan Basin; SSB, South Shetland Block; SOM, South Orkney Microcontinent; SOT; South Orkney Trench. Overlapped a simplification of the circulation of the regional deep and bottom water masses (compiled from: Orsi et al., 1999; Naveira-Garabato et al., 2002, 2007). Water masses: ACC, Antarctic Circumpolar Current; CDW, Circumpolar Deep Water; WSBW, Weddell Sea Bottom Water; WSDW, Weddell Sea Deep Water. Red dots mark the deepest passages for deep flow to (south) and from (north) the Scotia Sea. Climatological trajectory of the Polar Front (PF), such as defined by Orsi et al. (1995) and Naveira-Garabato et al. (2002). The red square outlines the study area.

Figure 2.- Multichannel seismic profiles dataset in the south Scotia Sea (see location in Fig. 1) acquired by Spanish Antarctic Research Group (Spanish), available in the Seismic Data Library System (SDLS), and old seismic data from British Antarctic Survey (BAS). The blue squares mark the location of the seismic sections shown in Fig. 4.

Figure 3.- South Scotia Sea: A) Simplified structural map of south Scotia Sea enhancing the main tectonic elements of the basins over bathymetric map based on Global Multi-Resolution Topography (GMRT) database (Ryan et al., 2009). SOT, South Orkney Trench. B) Bathymetric profile across the southern Scotia Sea basins –location marked in A by the yellow line. C) Regional two-way travel-time (TWTT) depth below sea level of the basement. D) Total sedimentary TWTT thickness in the region. The blue line represents the location of the profiles shown in Fig. 5.

Figure 4.- Segments of multichannel seismic profiles showing significant regional tectonic and stratigraphic structures: A) SCAN2004_SC03 across Scan Basin showing a detail of the interpreted dipping reflectors. B) SCAN2004_SC07 across the Dove Basin – Bruce Bank margin illustrating the tilted reflections related to the subsidence event after Reflector-c formation. See location in Fig. 2.

Figure 5.- Composite profile through the southern Scotia Sea basins formed by sections of the MCS profiles: TH97-06-1, IT89AW41, SCAN2013_SCS20, SCAN2001_SC08, SCAN2001_SC07, SCAN2001_SC10, SCAN2004_SC03, SCAN2004_SC04 and SCAN1997_SC12 (from west to east). See figure 3D for location. C/O B, Continent Ocean Boundary. Notice the interpretations include Pre- and Syn-rift deposits and Reflector-a’ not discussed in the present work. More details of these features can be found in Pérez et al. (2014a, 2014b, 2017).

Figure 6.- Regional sedimentary distribution of the identified sedimentary packages. A) Package-1 including seismic units above Reflector-c: III, II, I. B) Package-2 including seismic units between Reflector-e and Reflector-c: V, IV. C) Package-3 including seismic units below Reflector-e: VIII, VII, VI. Thickness in two-way travel-time (TWTT).

Figure 7.- Regional sedimentary distribution of the seismic units identified in all the southern Scotia Sea basins (Packages -1 and -2). Thickness in two-way travel-time (TWTT). Inferred flow of the

regional bottom water masses is overlapped: CDW, Circumpolar Deep Water; WSDW Weddell Sea Deep Water.

Figure 8.- Sketch reconstructions of the Scotia Sea formation. APR, Antarctic-Phoenix Ridge; DB, Dove Basin; EOB, East Ona Basin, ESR, East Scotia Ridge; JB, Jane Basin; PiB, Pirie Basin; PB, Powell Basin; PrB, Protector Basin; SB, Scan Basin; SFZ, Shackleton Fracture Zone; SSA, South Sandwich Arc; SST, South Sandwich Trench; WOB, West Ona Basin; WSR, West Scotia Ridge – W6 and W7 segments of the WSR. The orange star marks the approximate location of the Starfish structure according to Dalziel et al. (2013b). A to F represent distinct times from Paleocene to Present-day corresponding with the profiles in Fig. 9, whose theoretical location is marked by the dark blue line.

Figure 9.- Sketch profiles of the formation of the southern Scotia Sea basins. Profiles A to F represent distinct times from Paleocene to Present-day and correspond with the plan view reconstruction stages in Fig. 8. Tentative location of the profiles and acronyms are explained in Fig. 8.

Figure 10.- Synthetic sketch of the stratigraphic column along the southern Scotia Sea basins. The major regional stratigraphic changes and evolutionary phases are included.

Figure 11.- Integration of the study area´s sedimentary and tectonic sequences within a compilation of the main tectonic events (in red) discussed in this work at regional and Southern Hemisphere scales according to: Fiztgeral (1992), Rodríguez-Fernández et al. (1997), Bohoyo et al. (2002), Larter et al. (2003), Lawver and Gahagan (2003), Nisancioglu et al. (2003), Eagles et al. (2005), Livermore et al. (2005), Galindo-Zaldivar et al. (2006, 2014), Maldonado et al. (2006, 2014), Barker et al. (2013), Chatterjee et al. (2013), Hamon et al., 2013, Eagles and Jokat (2014), Schreider et al. (2018). CAS, Central American Seaway. The green bars mark periods of active compression in the Andean Cordillera (Torres-Carbonell et al., 2014). The context of the global glaciations and oxygen-isotope curve is based on Zachos et al. (2008). The eustatic curves are from Miller et al. (2005) (light purple) and Kominz et al. (2008) (dark purple). The connection of the main oceanic basins in the Southern Hemisphere to Antarctic Bottom Water (AABW) is pointed out (based on Carter and McCave (1994)). EECO, Early Eocene Climate Optimum; LMW, Late Miocene Warmth; LPTM, Late Paleocene Thermal Maximum; MECO, Mid-Eocene Climate Optimum;

MMCO, Mid-Miocene Climate Optimum; MMCT, Mid-Miocene Climate Transition; MPCT, Mid-Pliocene Climate Transition.

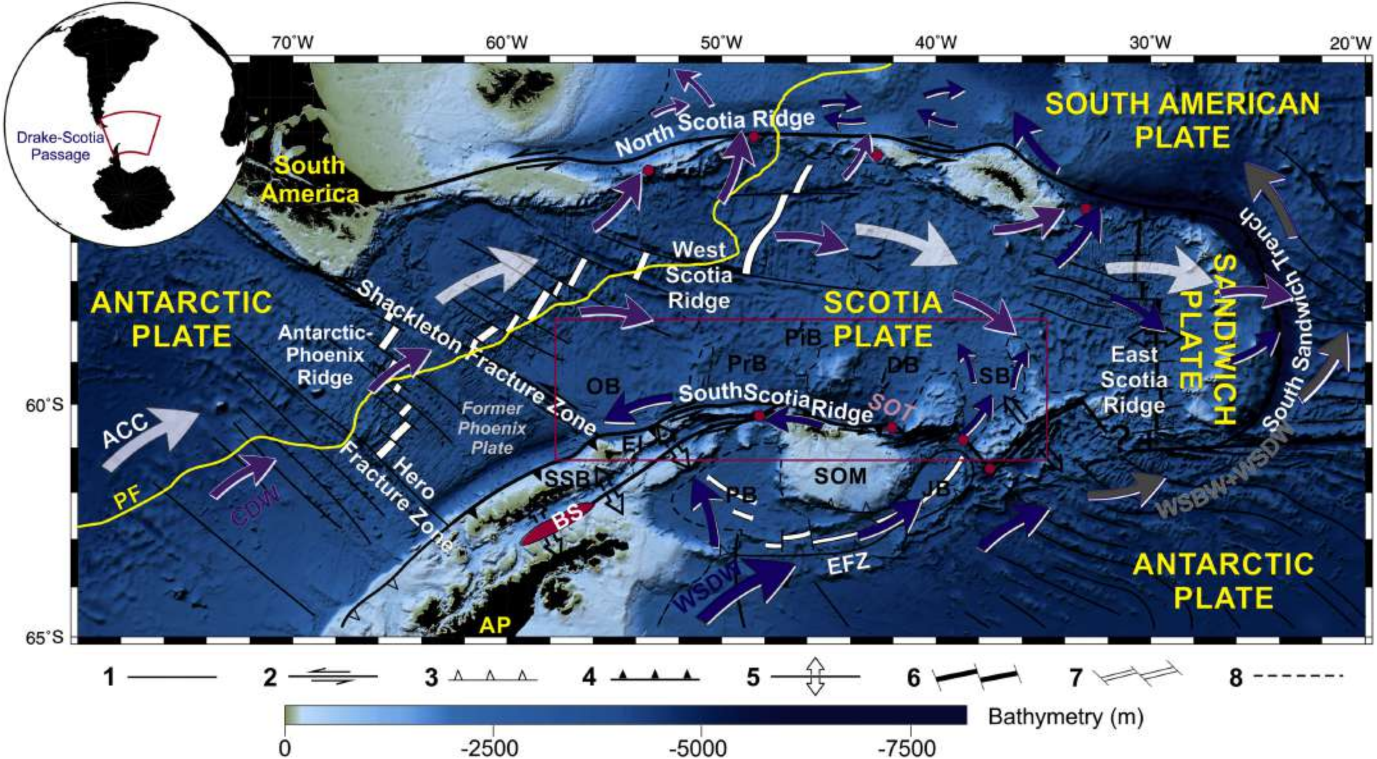
Drake-Scotia Passage
70°W
60°W
50°W
40°W
30°W
20°W
60°S
65°S
South America
SOUTH AMERICAN PLATE
North Scotia Ridge
West Scotia Ridge
ANTARCTIC PLATE
Antarctic-Phoenix Ridge
Shackleton Fracture Zone
SCOTIA PLATE
SANDWICH PLATE
South Sandwich Trench
East Scotia Ridge
PiB
PrB
DB
OB
SB
South Scotia Ridge
SOT
Former Phoenix Plate
ACC
PF
CDW
Hero Fracture Zone
EI
SSB
BS
PB
SOM
JB
EFZ
WSDW
WSBW+WSDW
AP
ANTARCTIC PLATE
1
2
3
4
5
6
7
8
Bathymetry (m)
0
-2500
-5000
-7500

Figure 1

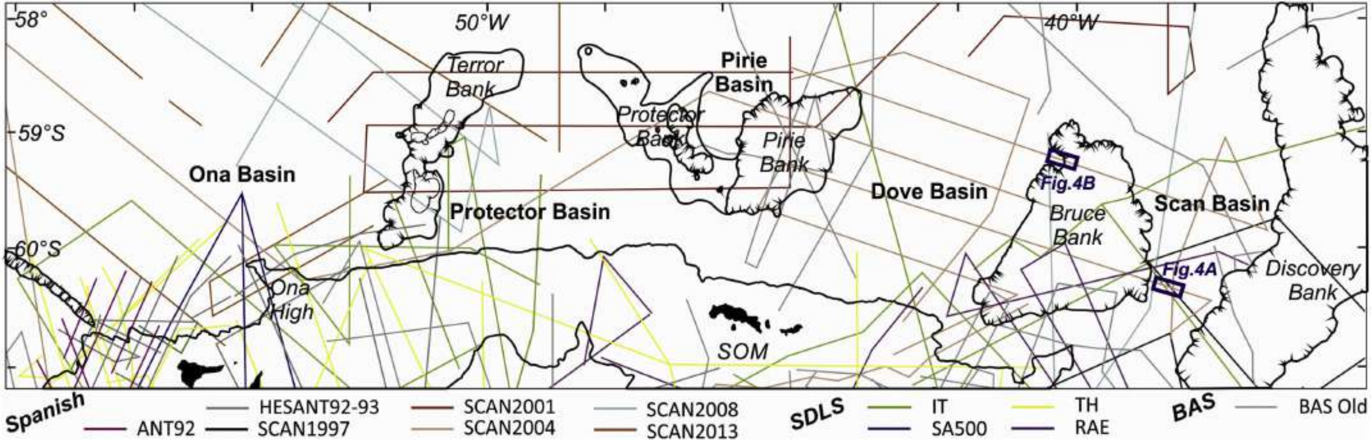

58°
50°W
40°W
59°S
60°S
Terror Bank
Pirie Basin
Protector Bank
Pirie Bank
Ona Basin
Protector Basin
Dove Basin
Fig.4B
Scan Basin
Bruce Bank
Fig.4A
Discovery Bank
Ona High
SOM
Spanish
ANT92
HESANT92-93
SCAN1997
SCAN2001
SCAN2004
SCAN2008
SCAN2013
SDLS
IT
SA500
TH
RAE
BAS
BAS Old

Figure 2

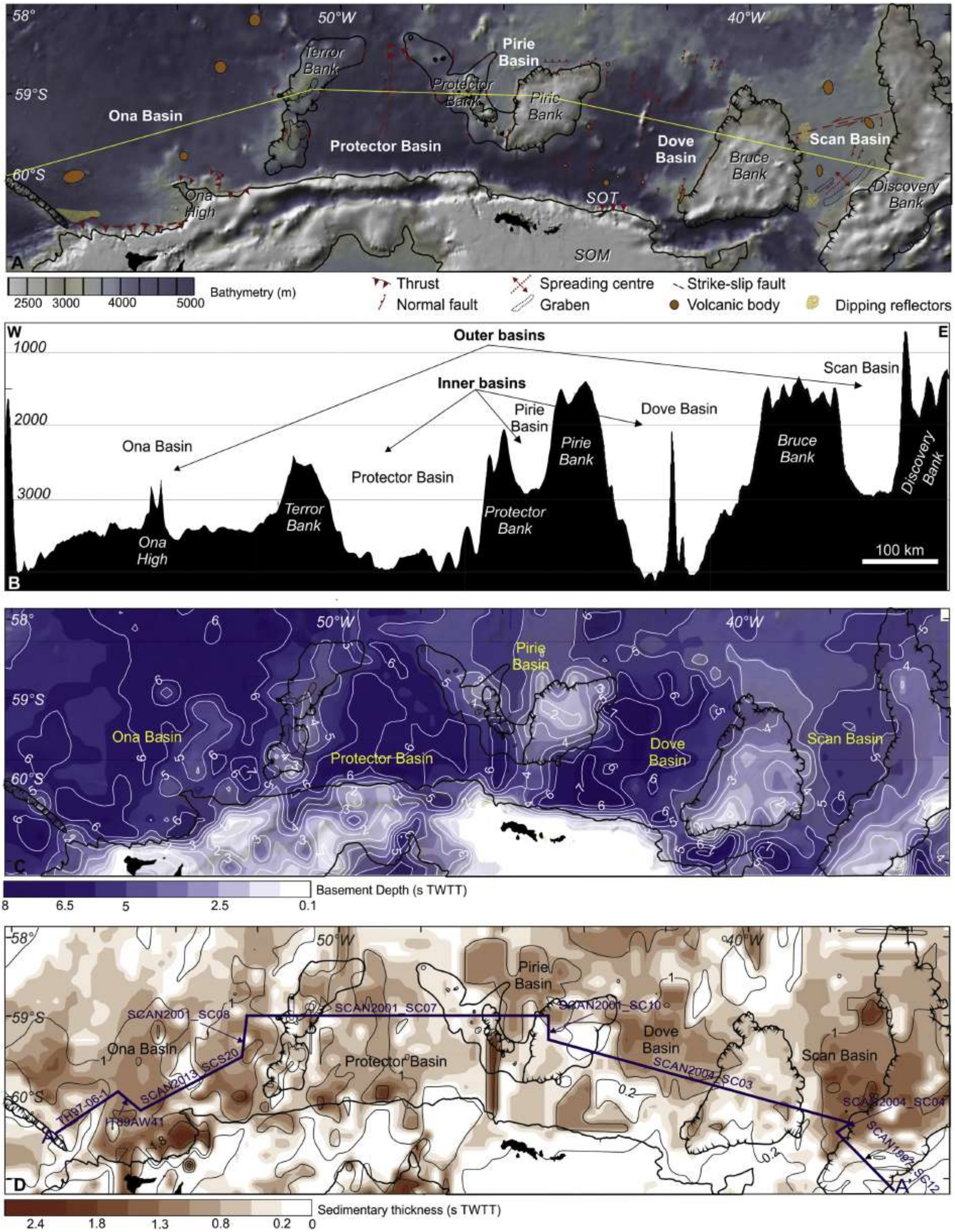

58°
50°W
40°W
59°S
60°S
Terror Bank
Pirie Basin
Protector Bank
Pirie Bank
Ona Basin
Protector Basin
Dove Basin
Bruce Bank
Scan Basin
Discovery Bank
Ona High
SOT
SOM
A
Bathymetry (m)
2500 3000 4000 5000
Thrust
Normal fault
Spreading centre
Graben
Strike-slip fault
Volcanic body
Dipping reflectors
W
E
1000
2000
3000
Outer basins
Inner basins
Ona Basin
Protector Basin
Pirie Basin
Dove Basin
Scan Basin
Terror Bank
Ona High
Protector Bank
Pirie Bank
Bruce Bank
Discovery Bank
100 km
B
C
Basement Depth (s TWTT)
8 6.5 5 2.5 0.1
D
SCAN2001_SC08
SCAN2001_SC07
SCAN2001_SC10
SCAN2013_SCS20
TH97-06-1
IT89AW41
SCAN2004_SC03
SCAN2004_SC04
SCAN1997_SC12
Sedimentary thickness (s TWTT)
2.4 1.8 1.3 0.8 0.2 0

Figure 3

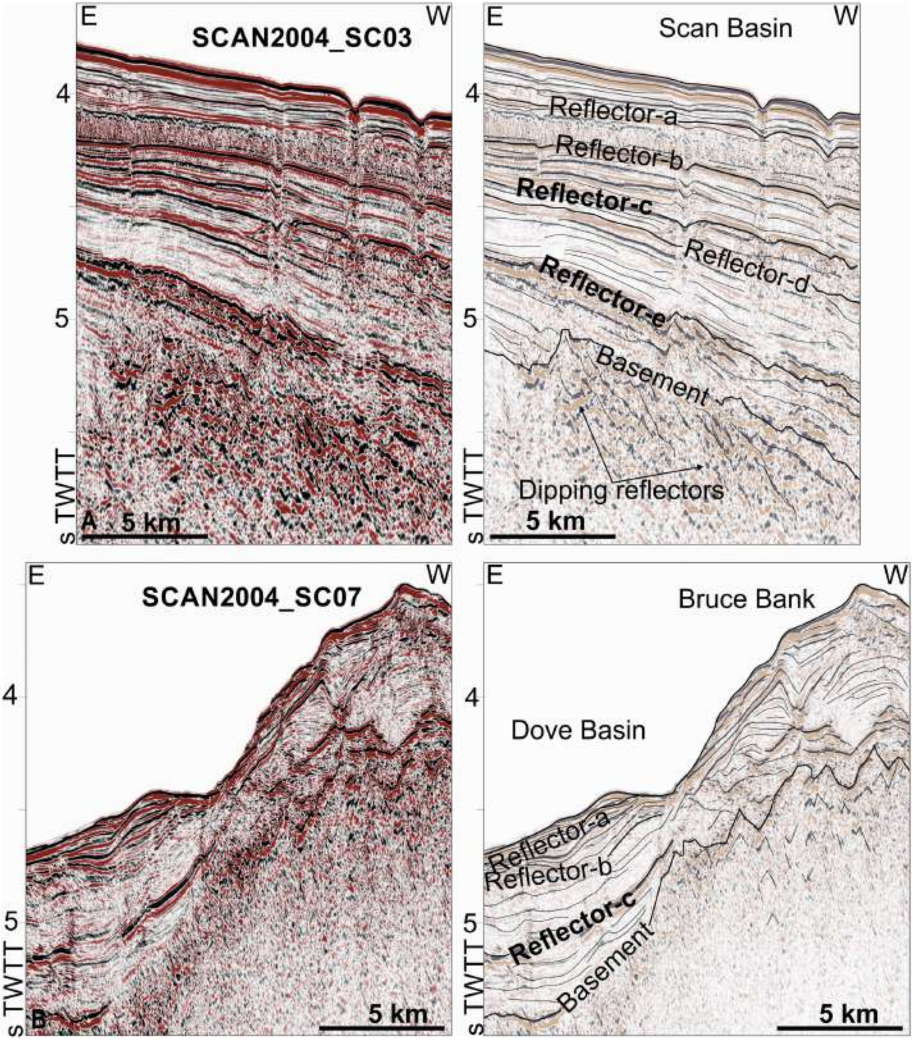
E
W
SCAN2004_SC03
4
5
s TWTT
A 5 km
E
W
Scan Basin
4
Reflector-a
Reflector-b
Reflector-c
Reflector-d
Reflector-e
5
Basement
Dipping reflectors
s TWTT
5 km
E
W
SCAN2004_SC07
4
5
s TWTT
B
5 km
E
W
Bruce Bank
4
Dove Basin
Reflector-a
Reflector-b
Reflector-c
5
Basement
s TWTT
5 km

Figure 4

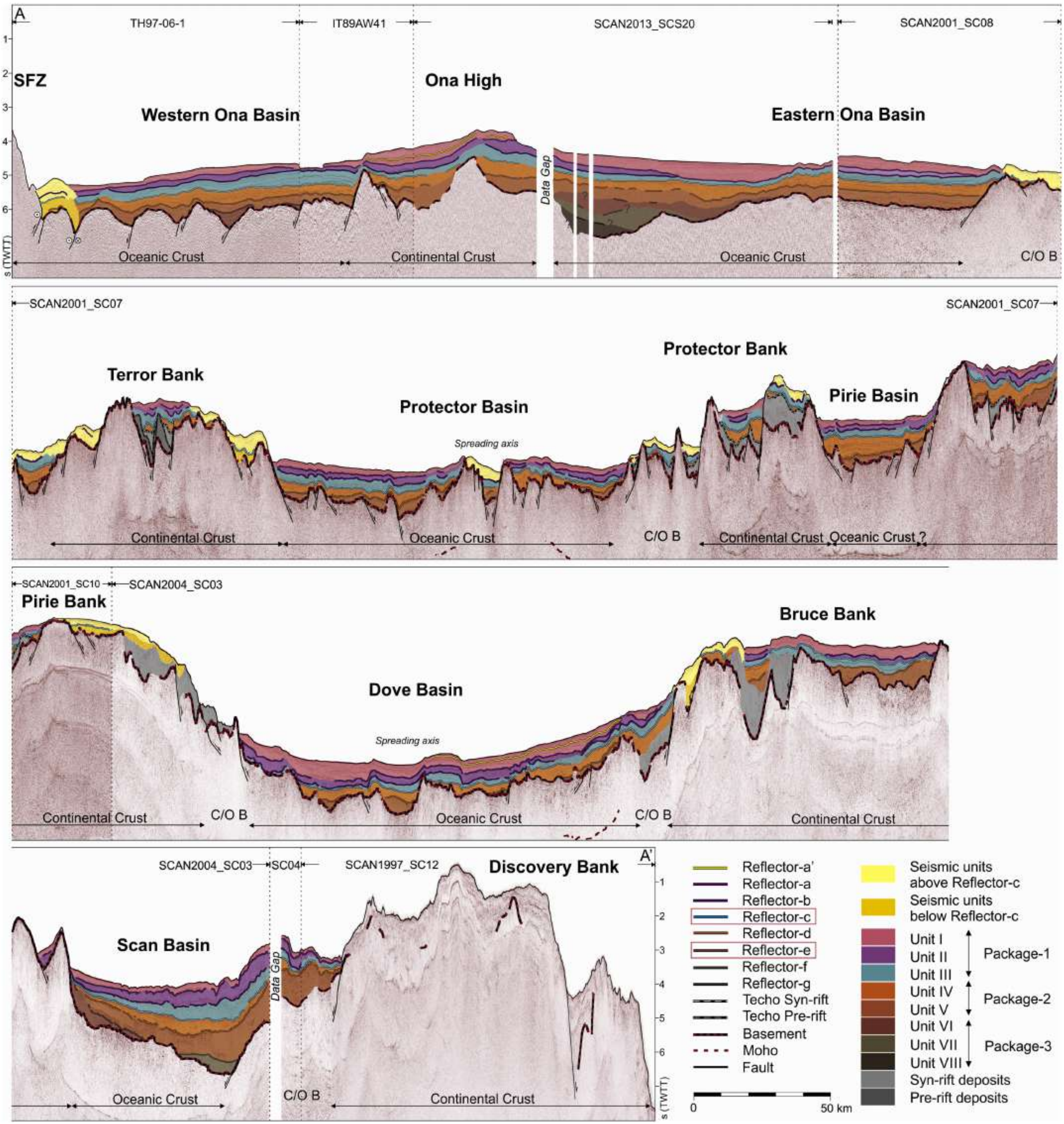
A
TH97-06-1
IT89AW41
SCAN2013_SCS20
SCAN2001_SC08
SFZ
Western Ona Basin
Ona High
Eastern Ona Basin
Data Gap
Oceanic Crust
Continental Crust
Oceanic Crust
C/O B
s (TWTT)
SCAN2001_SC07
SCAN2001_SC07
Terror Bank
Protector Bank
Protector Basin
Pirie Basin
Spreading axis
Continental Crust
Oceanic Crust
C/O B
Continental Crust
Oceanic Crust ?
SCAN2001_SC10
SCAN2004_SC03
Pirie Bank
Bruce Bank
Dove Basin
Spreading axis
Continental Crust
C/O B
Oceanic Crust
C/O B
Continental Crust
SCAN2004_SC03
SC04
SCAN1997_SC12
A'
Discovery Bank
Scan Basin
Data Gap
Oceanic Crust
C/O B
Continental Crust
s (TWTT)
Reflector-a'
Reflector-a
Reflector-b
Reflector-c
Reflector-d
Reflector-e
Reflector-f
Reflector-g
Techo Syn-rift
Techo Pre-rift
Basement
Moho
Fault
0
50 km
Seismic units above Reflector-c
Seismic units below Reflector-c
Unit I
Unit II
Unit III
Package-1
Unit IV
Unit V
Package-2
Unit VI
Unit VII
Unit VIII
Package-3
Syn-rift deposits
Pre-rift deposits

Figure 5

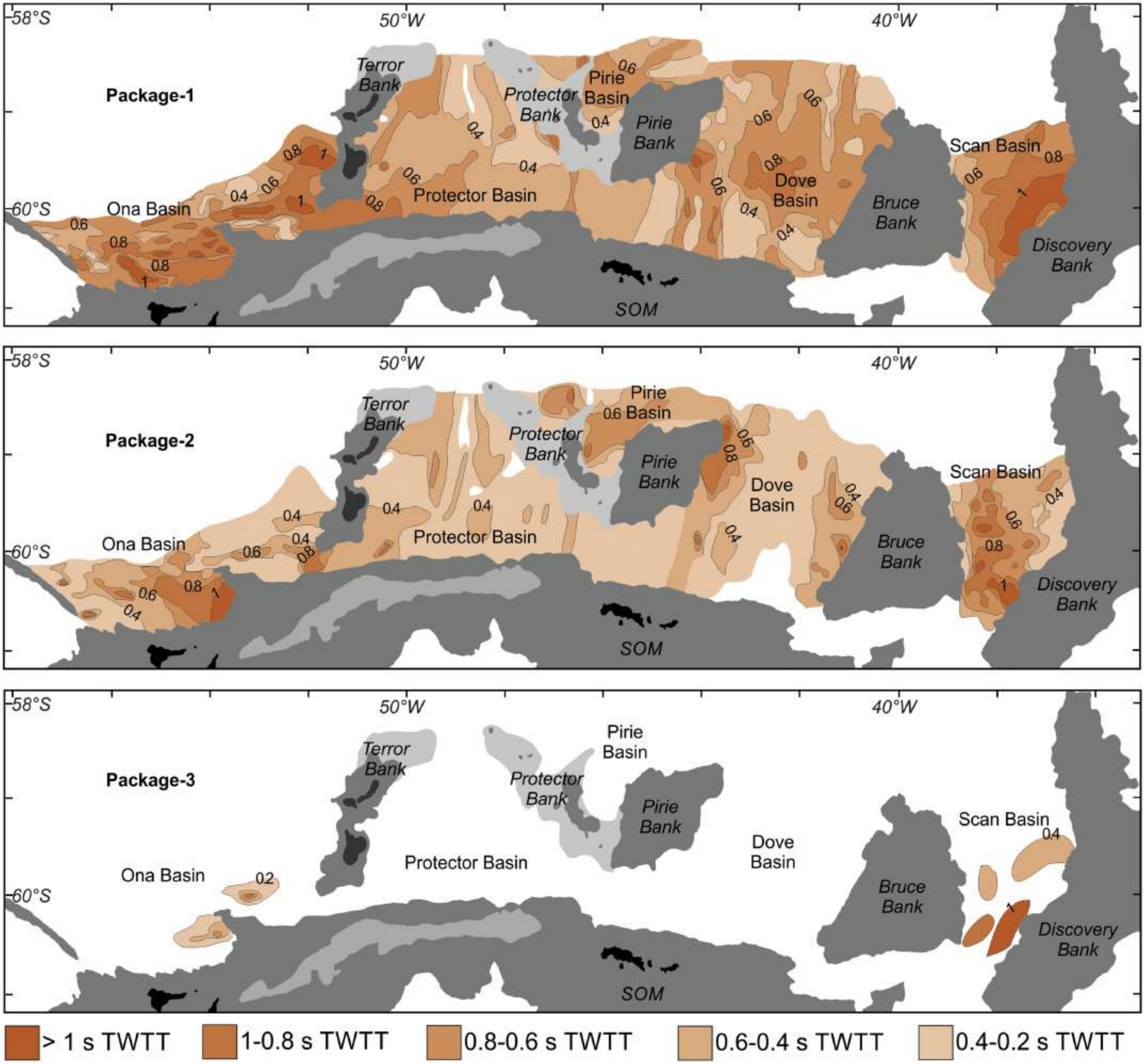

58°S
50°W
40°W
60°S
Package-1
Terror Bank
Protector Bank
Pirie Basin
Pirie Bank
Scan Basin
Ona Basin
Protector Basin
Dove Basin
Bruce Bank
Discovery Bank
SOM
Package-2
Package-3
> 1 s TWTT
1-0.8 s TWTT
0.8-0.6 s TWTT
0.6-0.4 s TWTT
0.4-0.2 s TWTT

Figure 6

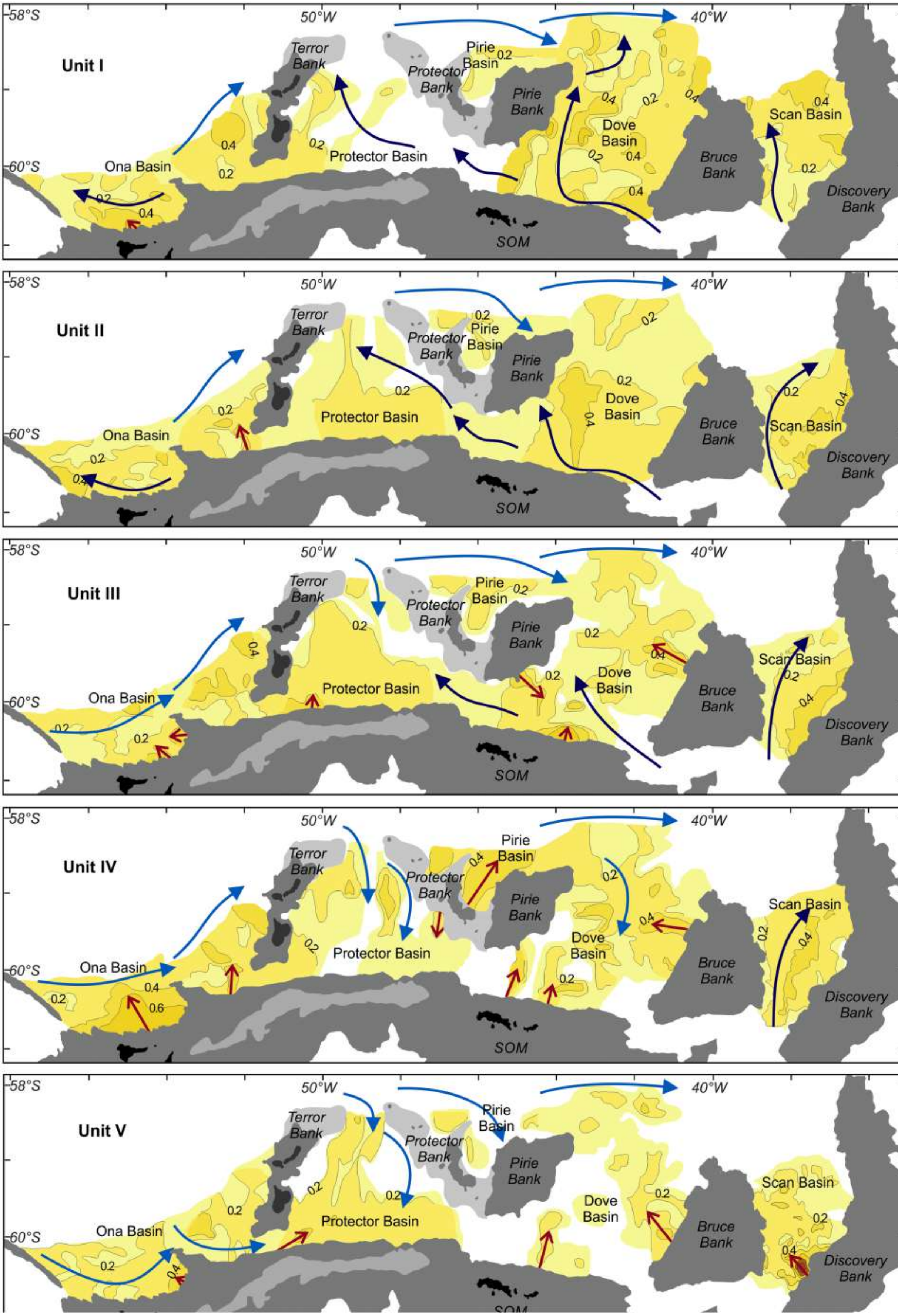
Unit I
Unit II
Unit III
Unit IV
Unit V
58°S
60°S
50°W
40°W
Terror Bank
Protector Bank
Pirie Basin
Pirie Bank
Protector Basin
Ona Basin
Dove Basin
Bruce Bank
Scan Basin
Discovery Bank
SOM
0.2
0.4
0.6

Figure 7

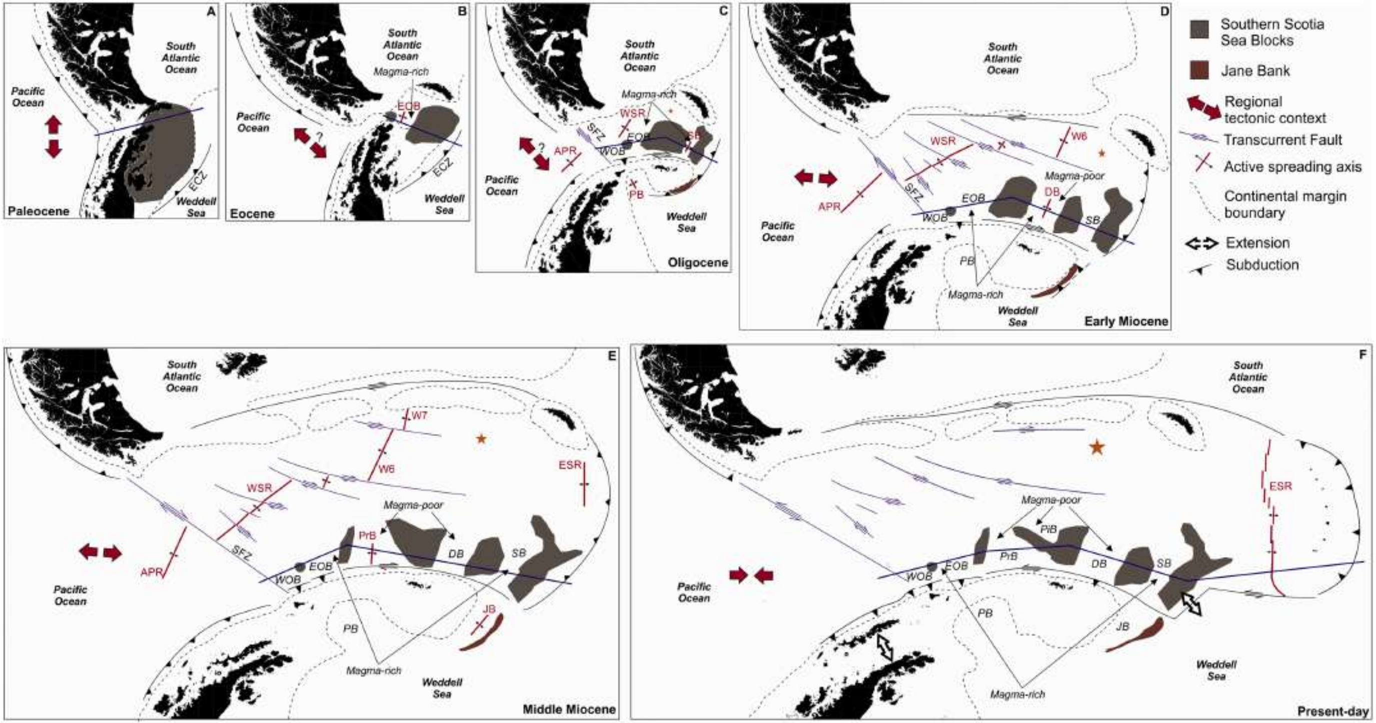
A
B
C
D
E
F
Paleocene
Eocene
Oligocene
Early Miocene
Middle Miocene
Present-day
South Atlantic Ocean
Pacific Ocean
Weddell Sea
ECZ
Magma-rich
Magma-poor
EOB
WOB
WSR
SFZ
APR
PB
SR
DB
SB
W6
W7
ESR
PrB
PiB
JB
Southern Scotia Sea Blocks
Jane Bank
Regional tectonic context
Transcurrent Fault
Active spreading axis
Continental margin boundary
Extension
Subduction

Figure 8

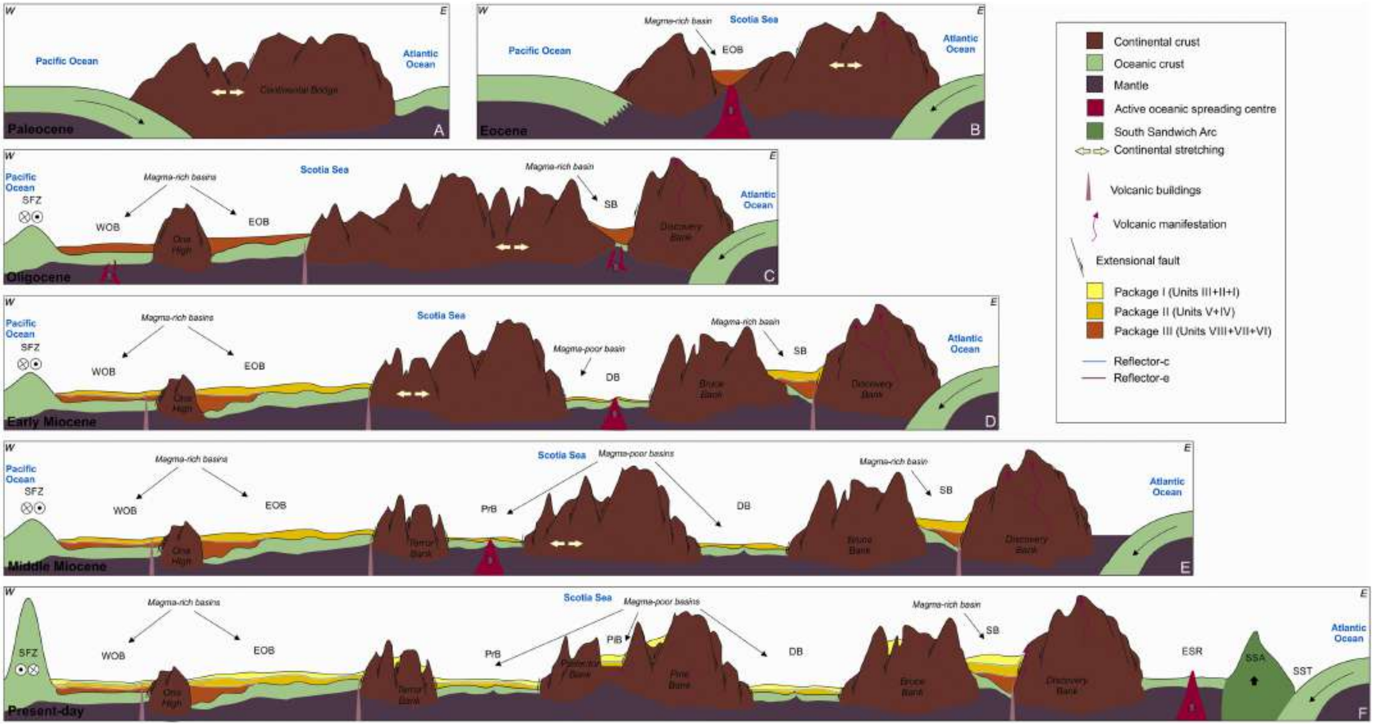

Paleocene
Pacific Ocean
Atlantic Ocean
Continental Bridge
Eocene
Magma-rich basin
Scotia Sea
EOB
Oligocene
Magma-rich basins
WOB
SFZ
Ona High
SB
Discovery Bank
Early Miocene
Magma-poor basin
DB
Bruce Bank
Middle Miocene
Magma-poor basins
PrB
Terror Bank
Present-day
PiB
Protector Bank
Pirie Bank
ESR
SSA
SST
Continental crust
Oceanic crust
Mantle
Active oceanic spreading centre
South Sandwich Arc
Continental stretching
Volcanic buildings
Volcanic manifestation
Extensional fault
Package I (Units III+II+I)
Package II (Units V+IV)
Package III (Units VIII+VII+VI)
Reflector-c
Reflector-e

Figure 9

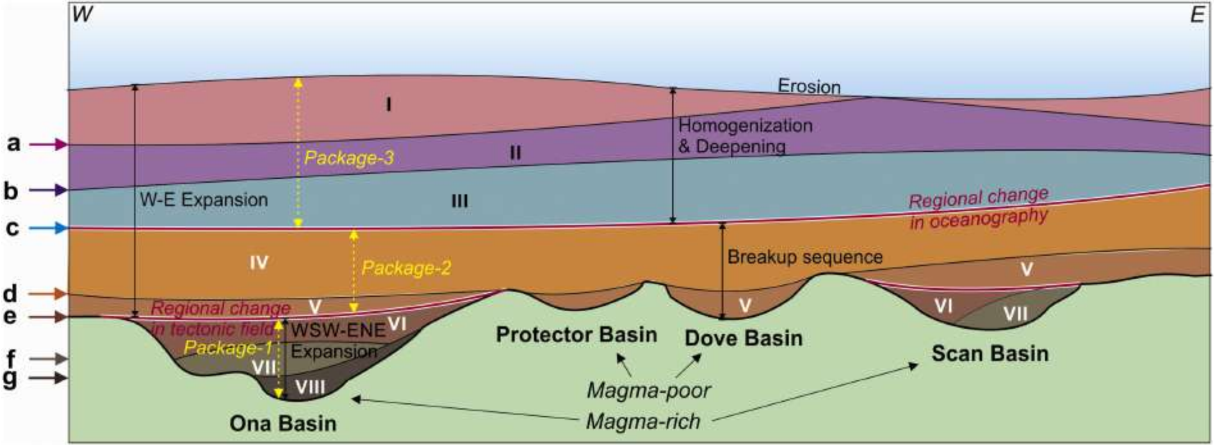
W
E
Erosion
I
Homogenization
& Deepening
II
Package-3
a
b
W-E Expansion
III
c
Regional change
in oceanography
IV
Package-2
Breakup sequence
V
d
e
V
Regional change
in tectonic field
V
WSW-ENE
Expansion
VI
Package-1
VII
VIII
f
g
Protector Basin
Dove Basin
VI
VII
Scan Basin
Magma-poor
Magma-rich
Ona Basin

Figure 10

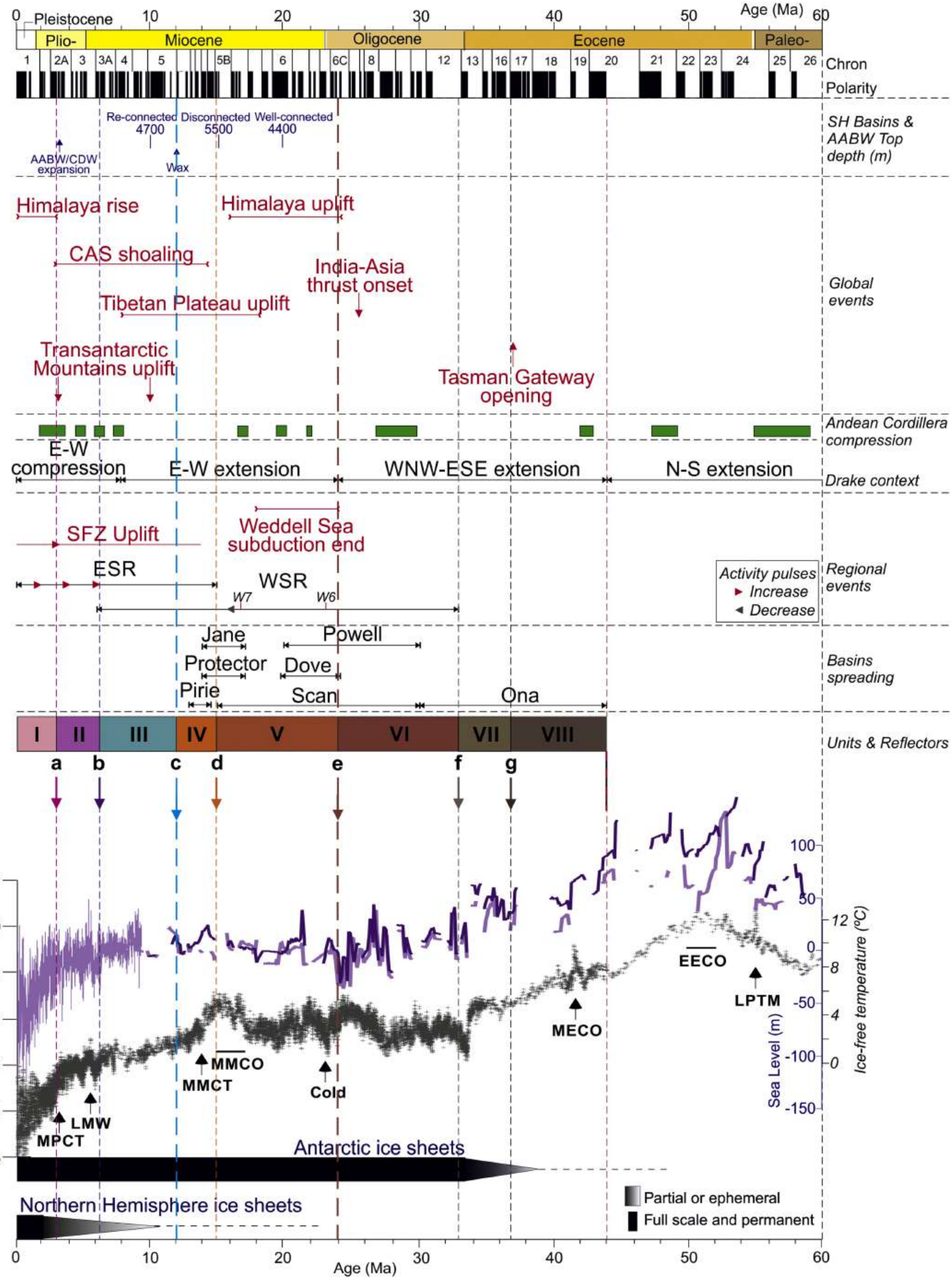

Pleistocene
Age (Ma)
Plio-
Miocene
Oligocene
Eocene
Paleo-
Chron
Polarity
SH Basins & AABW Top depth (m)
Re-connected
Disconnected
Well-connected
4700
5500
4400
AABW/CDW expansion
Wax
Himalaya rise
Himalaya uplift
CAS shoaling
India-Asia thrust onset
Tibetan Plateau uplift
Global events
Transantarctic Mountains uplift
Tasman Gateway opening
Andean Cordillera compression
E-W compression
E-W extension
WNW-ESE extension
N-S extension
Drake context
SFZ Uplift
Weddell Sea subduction end
ESR
WSR
W7
W6
Activity pulses
Increase
Decrease
Regional events
Jane
Powell
Protector
Dove
Pirie
Scan
Ona
Basins spreading
I
II
III
IV
V
VI
VII
VIII
Units & Reflectors
a
b
c
d
e
f
g
δ18O (‰)
Sea Level (m)
Ice-free temperature (ºC)
EECO
LPTM
MECO
MMCO
MMCT
Cold
LMW
MPCT
Antarctic ice sheets
Northern Hemisphere ice sheets
Partial or ephemeral
Full scale and permanent
Age (Ma)

Figure 11